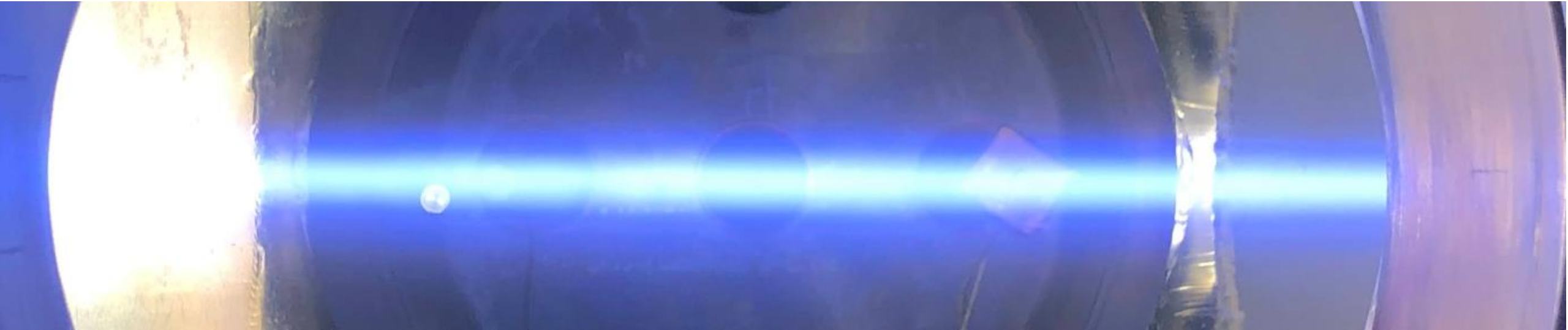


Magnetically-enhanced Plasma Sources for Materials Processing Applications



Yevgeny Raitses

Princeton Plasma Physics Laboratory

PPPL School on Plasmas for Microelectronics and QIS
Princeton, NJ
July 28-August 1, 2025

Outline

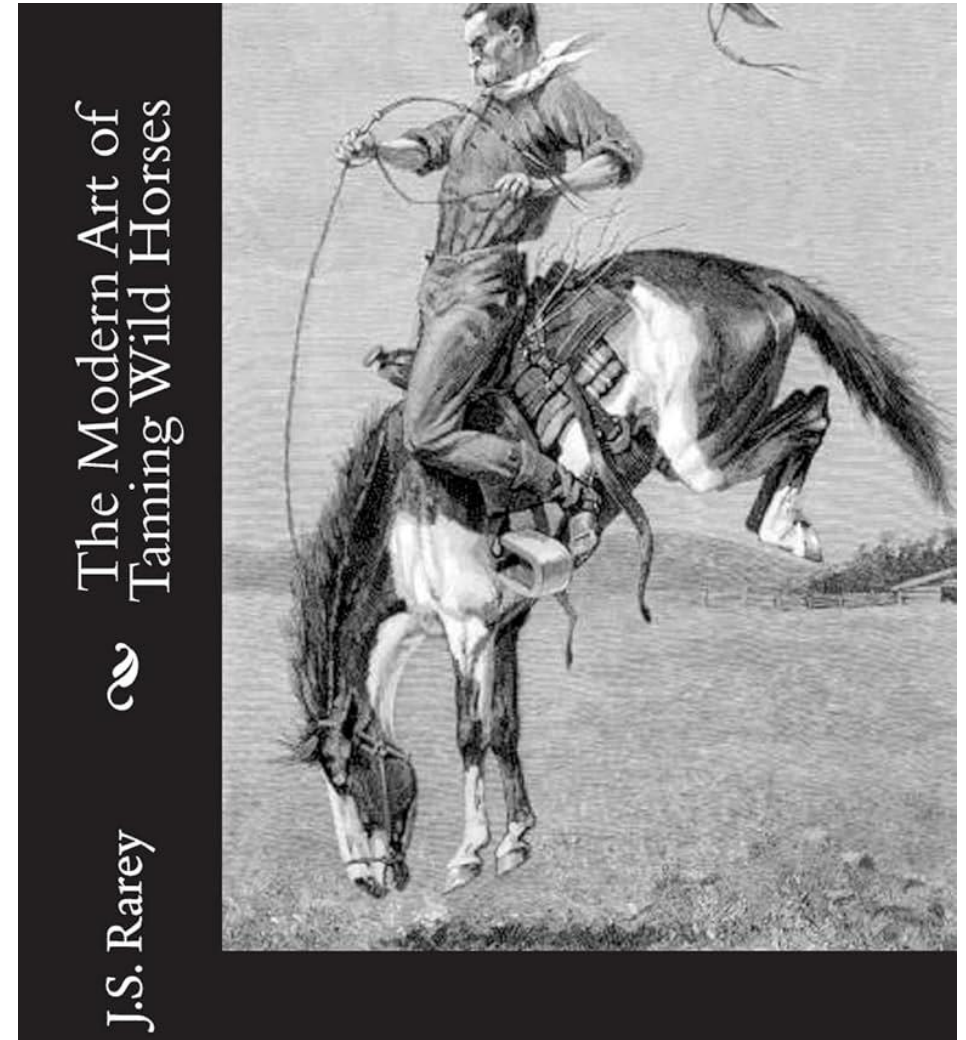
- Why magnetic field?
- Status quo: magnetically-enhanced plasma processing sources
- Magnetic field effects on charged particles and plasma
- Gentle processing of sensitive materials with $E \times B$ plasmas for emerging applications in nanoelectronics and QIS
- **Princeton Collaborative Low Temperature Plasma Research Facility (PCRF) 2026 Call for User Proposals**
<http://pcrf.pppl.gov>
yraitses@pppl.gov

Why magnetic field for low temperature plasma sources?

- Magnetically-enhanced low pressure (0.1-10's mtorr) low temperature plasma (LTP) sources for processing— **Confine & Control**
- Magnetic field confines plasma (in the direction perpendicular to the magnetic field)
- Magnetic field provides additional options to control plasma
 - Qualitatively new regimes, new (often unique) applications and new devices (e.g. ECR, magnetrons, e-beam ExB plasma in plasma processing, electric propulsion, ...)

New challenges and problems with magnetically-controlled plasmas

Complexity from anisotropy, instabilities, nonlinear interactions and their various consequences, e.g. turbulence and transport, plasma structures and arcing....



Anode Layer Ion Source

Applications

- Ion sputtering
- Ion cleaning and etching
- Ion beam assisted deposition
- Surface modifications
- Deposition of amorphous carbon and other materials

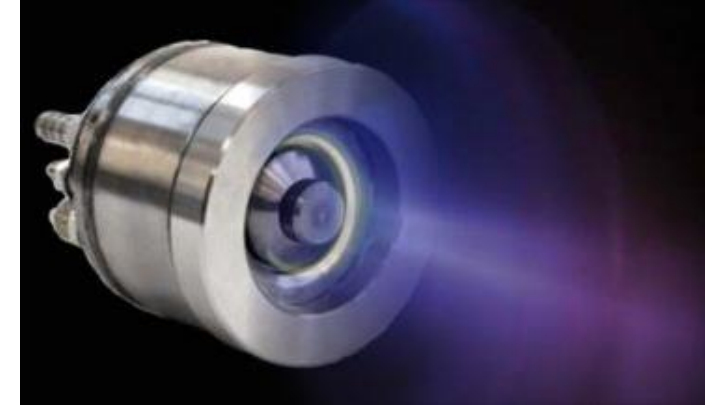
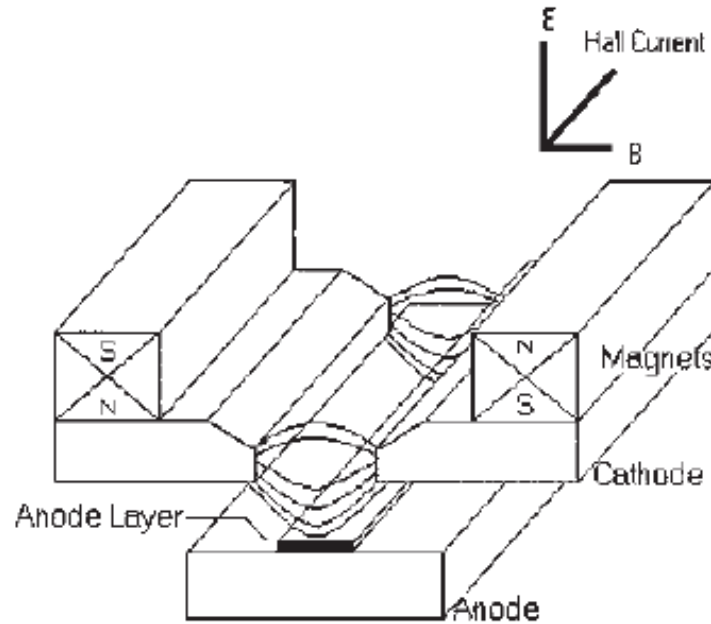


Table 1: Typical Discharge Parameters

| Parameter | Units | Value |
|----------------------------|---------|------------|
| Discharge Voltage Range | kV | 0.7 to 3.0 |
| Maximum Discharge Current* | ma/cm | 10 to 30 |
| Maximum Discharge Power* | W/cm | 33 to 100 |
| Operating Pressure Range | mTorr | 0.1 to 10 |
| Maximum Gas Flow* | sccm/cm | 3 |
| Cooling Water Flow | L/min | 2 |

Table 2: Typical Ion Beam Parameters

| Parameter | Units | Value |
|----------------------------|--------------------|-------------|
| Mean Energy | keV | 0.25 to 1.8 |
| Energy spread | % of Mean Energy | +/-15 |
| Maximum Current* | ma/cm | 10 to 30 |
| Maximum Power* | W/cm | 33 to 100 |
| Beam Divergence at 1 mTorr | Degrees half angle | 3 to 6 |



<https://www.beamtec.de/en/anode-layer-ion-sources/>

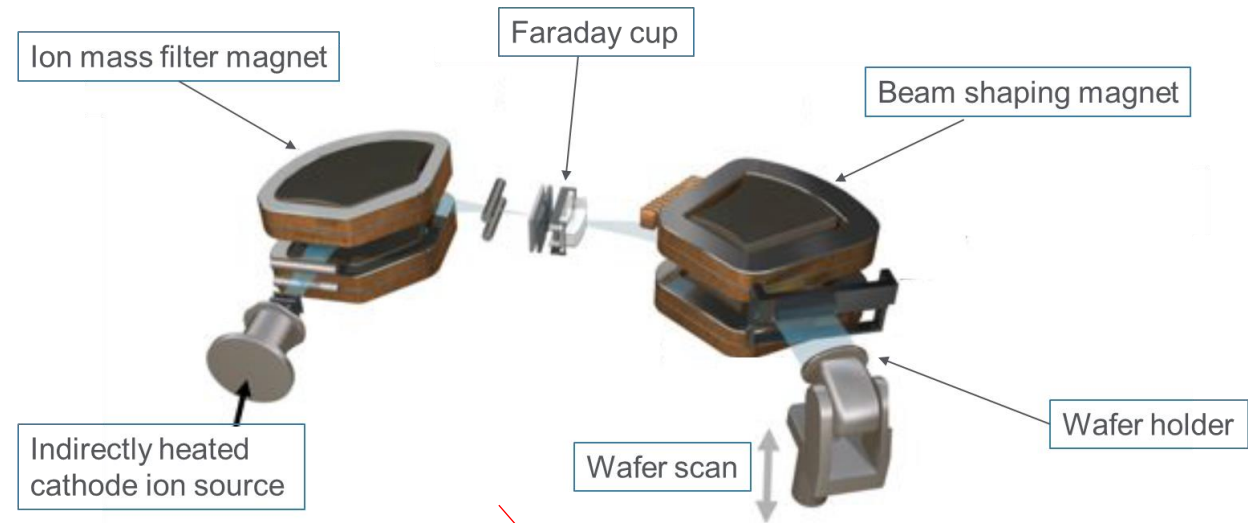
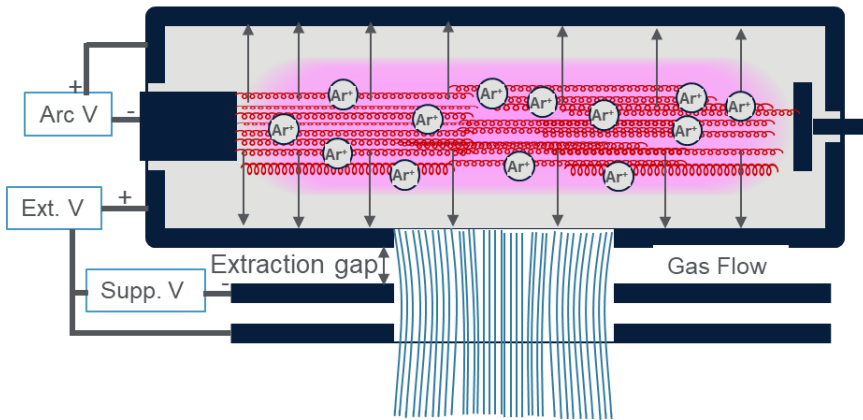
J.E. Keem, 44th Annual Technical Confer. Proc. (2001)

Ion implantation and Patterning (nm-scale)

Ion implantation is a materials modification technique where ions of a desired element are accelerated and implanted into a target material to alter its physical, chemical, or electrical properties.

Patterning – to print chip features on the wafer. Ion implanters to assist EUV lithography in reducing the feature size below the EUV scale.

Freeman and Barnas E×B Ion Sources

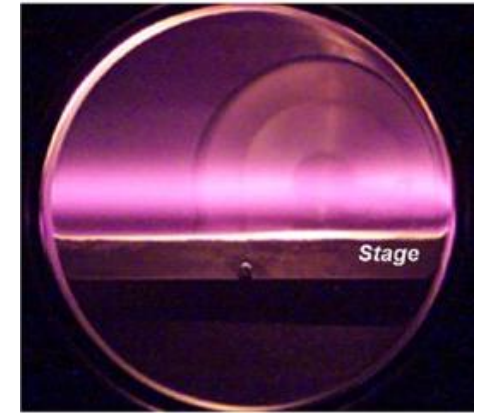
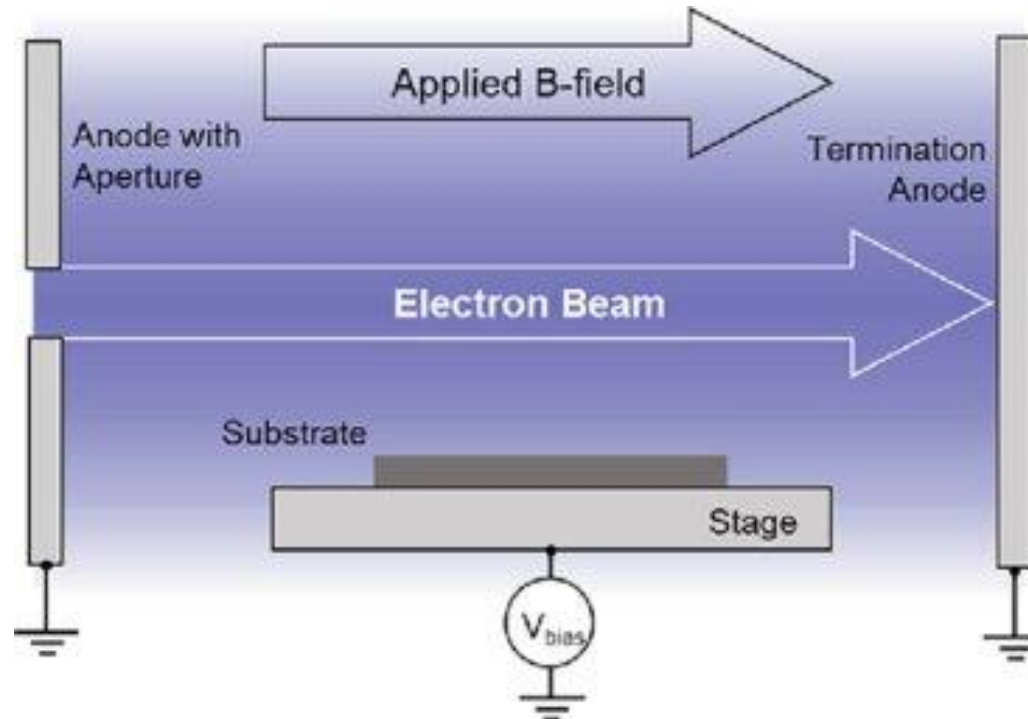


AMAT VISta® 3000XP

Electron-beam Generated (E×B) Plasma Sources

Gentle or Soft processing

- Doping
- Atomic Layer Etching
- Functionalization,
- Termination



W. M. Manheimer et al., Plasma Sources Sci. Technol. 9 (2000)

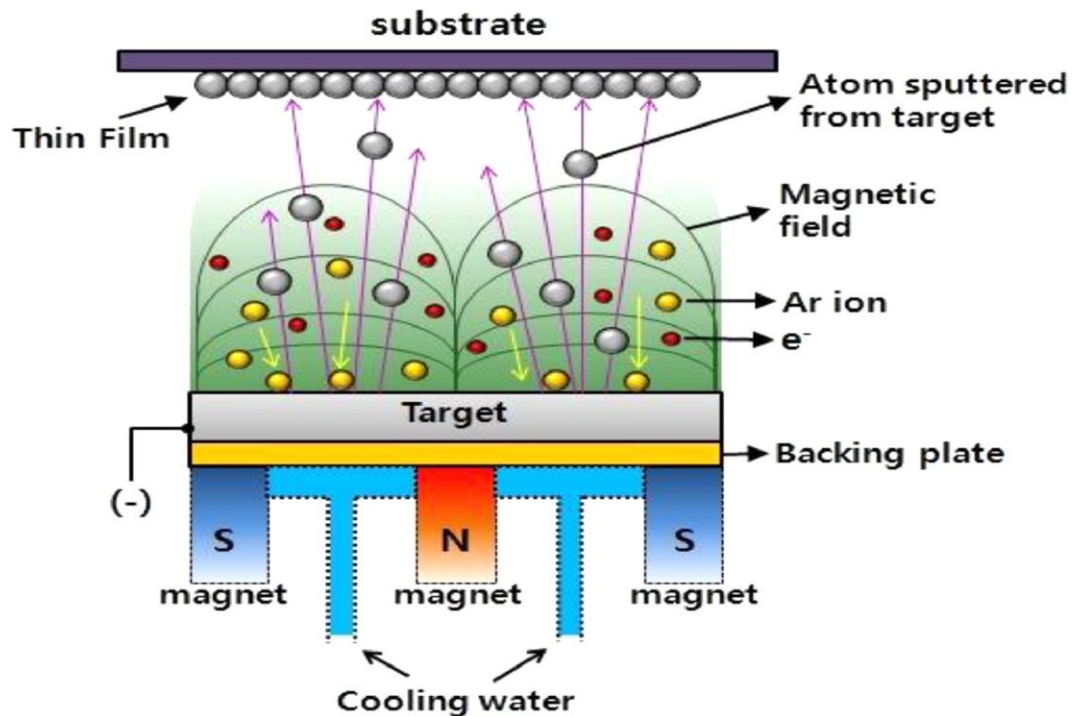
*S. Walton et al., Surf. Coat. Technol. **186** (2004)*

*F. Zhao et al., Carbon **177** (2021)*

We will discuss these sources more later in the talk.

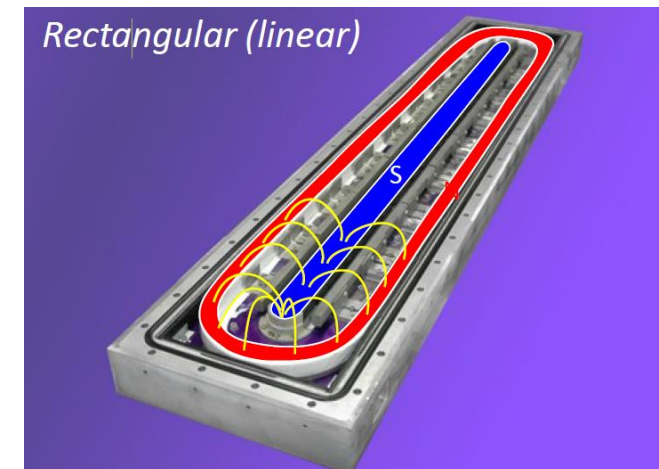
Sputtering Magnetrons: *DC, RF, High –power Impulse (Hi-PIMS)*

- Thin films in integrated circuits, photovoltaics
- Optical thin films,
- Protective coatings



Gas pressure range:
1-100 mtorr

B. Janarthanan et al., J. Mol. Struct. (2021)

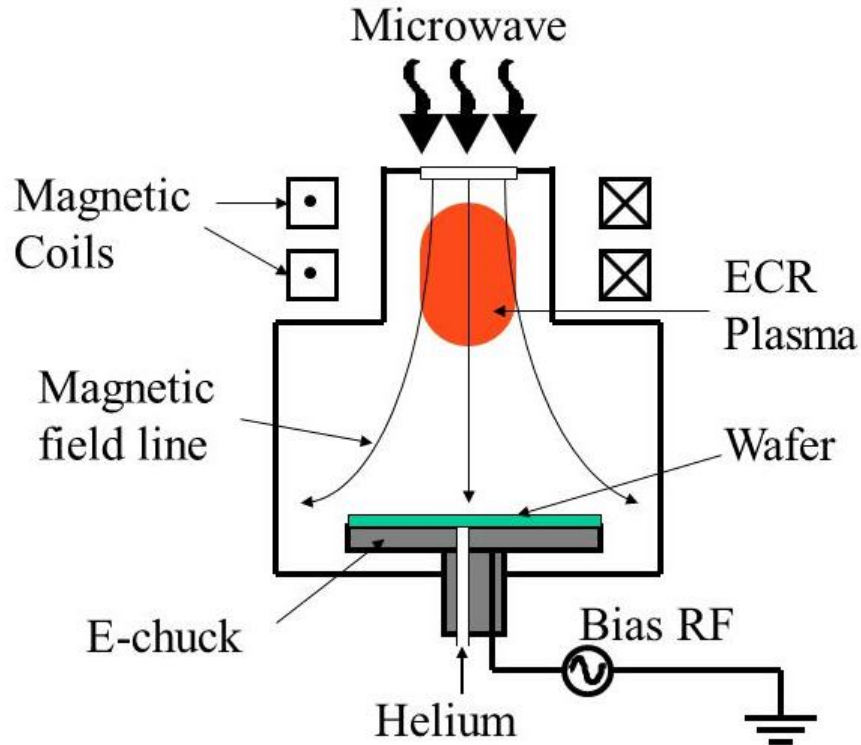


Courtesy Matjaž Panjan, Jožef Stefan Institute

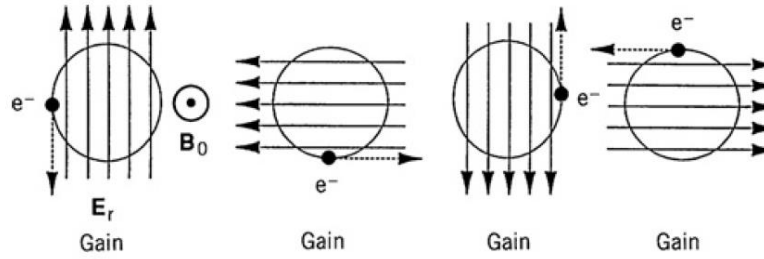
Electron Cyclotron Resonance (ECR) Plasma Sources

Applications:

-Etching and Deposition



Electrons are in resonance with circularly polarized electromagnetic wave



$$\mathbf{E} = E_0 (\mathbf{x} \cos \omega t + \mathbf{y} \sin \omega t)$$

$$\omega = \omega_{ec} \Rightarrow \text{Cyclotron resonance}$$

For 2.45 GHz, Magnetic field = 875 Gauss

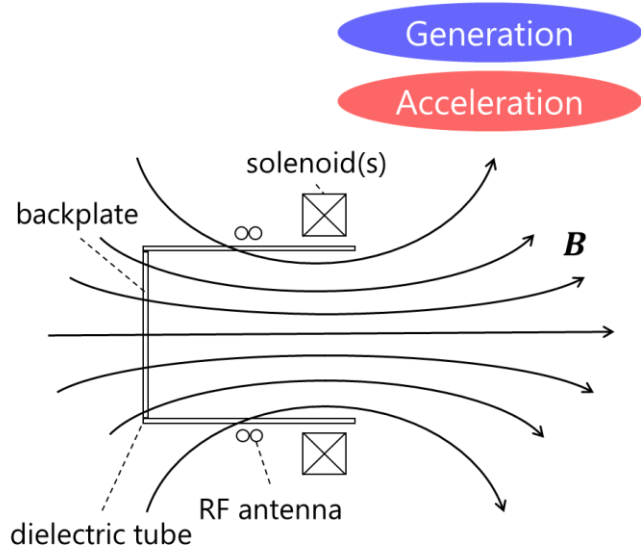
Gas pressure: 0.1-10 mtorr

Plasma density: 10^9 - 10^{12} cm⁻³

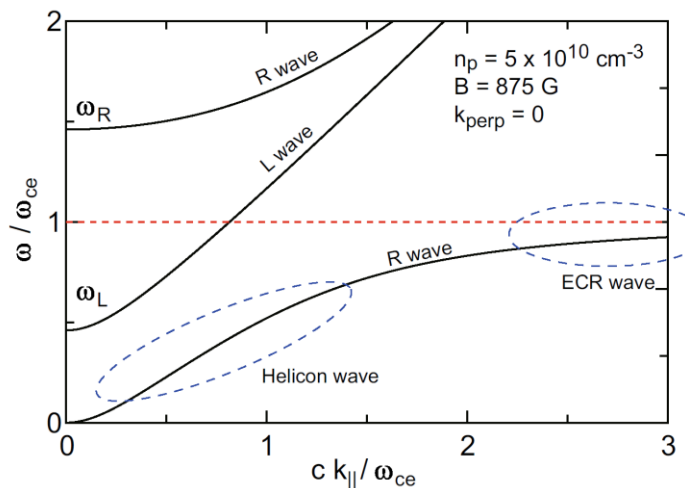


UHF-ECR by Hitachi

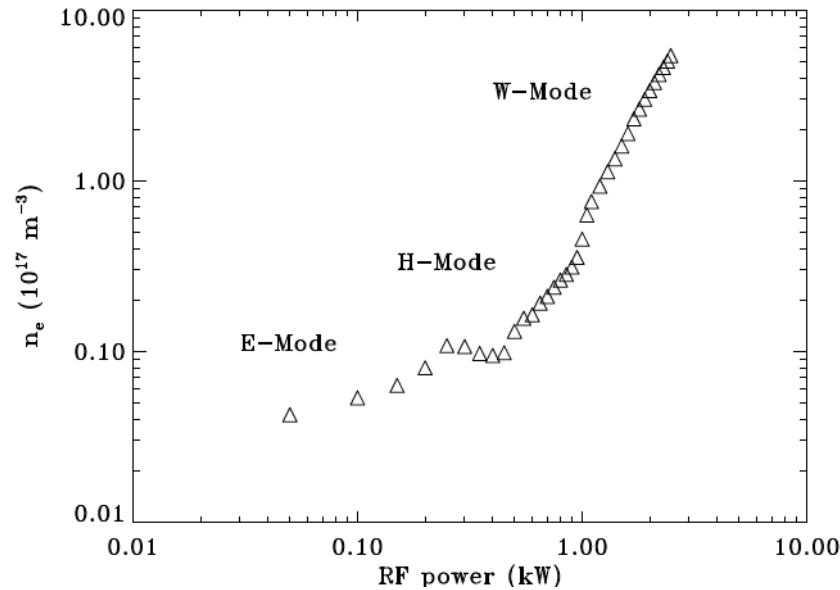
Helicon Plasma Sources



H. Sekine, IEPC-2022-523



K. Takahashi, Rev. Mod. Plasma Phys. **3** (2019)

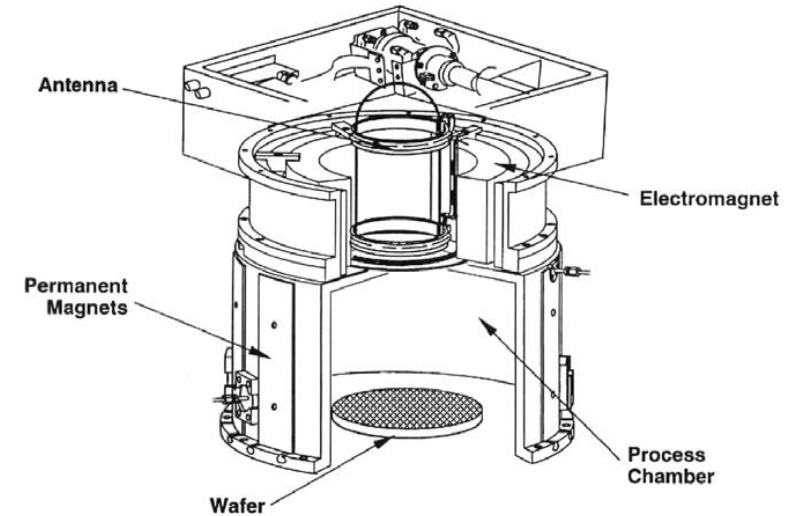


Measurements in WOMBAT
Courtesy Rod Boswell, ANU

In W-mode, the electrons are heated by helicon waves.

The helicon and ECR waves are essentially the whistler mode having the right-hand polarization and a resonance condition at $\omega = \omega_{ec}$

Trikon MORI TM 200 Plasma Etcher

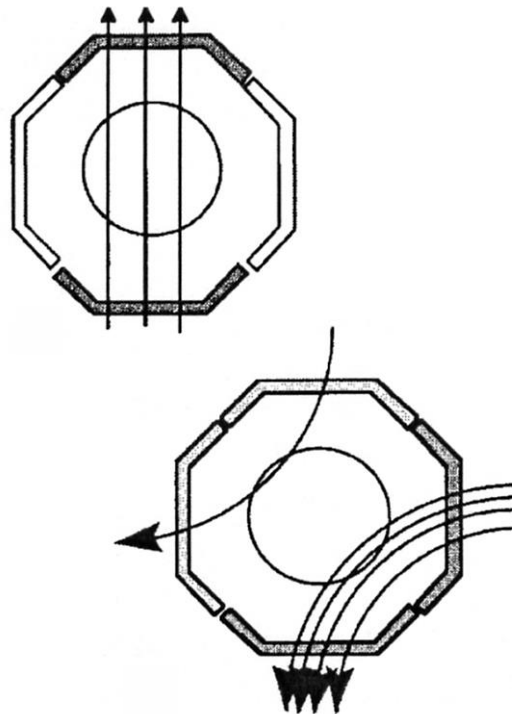
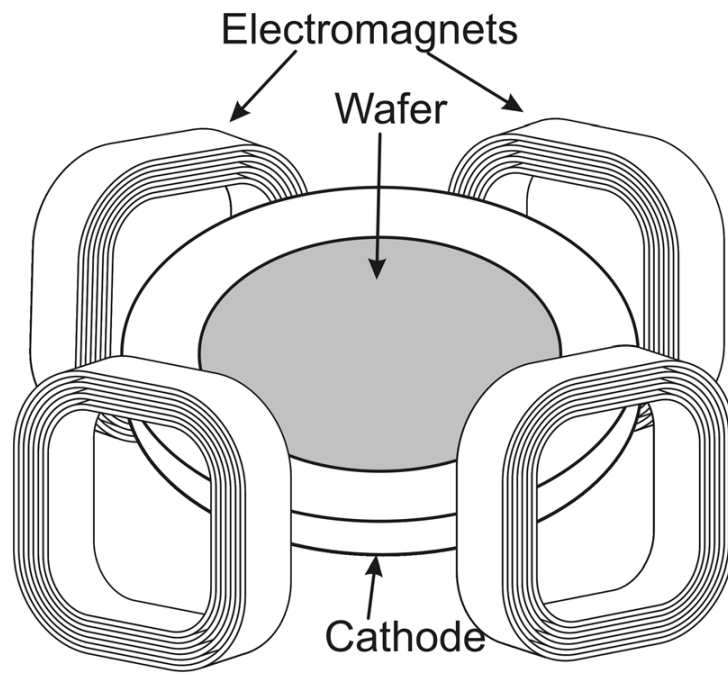


G. R. Tynan et al., J. Vac. Sci. Technol. A **15** (1997)

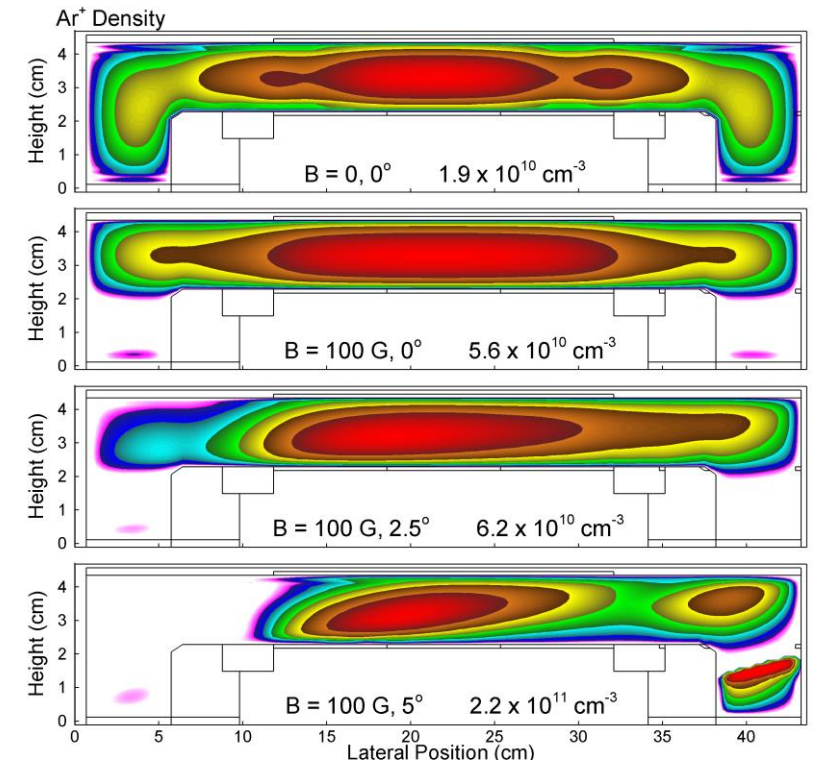
Magnetically –enhanced RF plasma sources for processing

Rotating Magnetic Field CCP Reactor

- Varied coil current in the four coils to generate a rotating B- field
- Rotating field averages out plasma non-uniformities



- Ar, 40 mTorr, 100 W, 10 MHz



Applied Materials MERIE RF CCP reactor

D. Cheng et al, US Patent **4**, 842,683 (1988)

M. Buie et al, JVST A **16** (1998)

N. Babaeva and M. Kushner, GEC 2008

Motion of charged particles in the magnetic field

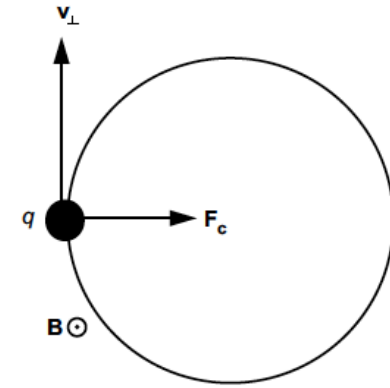
For $E = 0, B \neq 0$, Lorentz force maintains a circular orbit of a particle with charge, q :

$$\mathbf{F}_c = q\mathbf{v}_\perp \times \mathbf{B} = \frac{mv_\perp^2}{r} \quad \leftarrow \text{Centripetal force}$$

Larmor radius $r_L = \frac{mv_\perp}{qB} = \frac{v_\perp}{\omega_c}$

Cyclotron frequency

$$\omega_c = qB/m$$

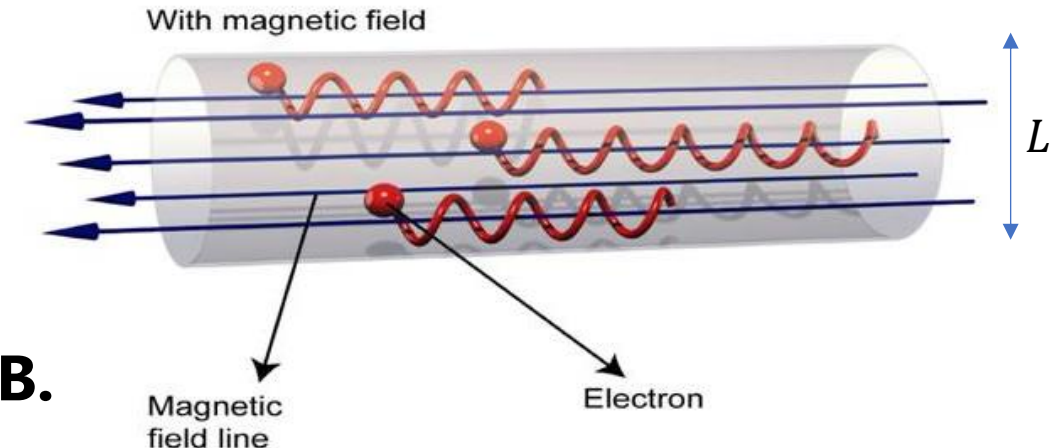


Charged species are magnetized if B-field is sufficiently strong:

$$r_L < L, \quad \omega_c > \nu$$

Particles are confined in the direction perpendicular to B , but can freely flow along B .

For typical magnetically-enhanced LTP electrons are magnetized while ions are not.



Particle motion in the inhomogeneous magnetic field

When a charged particle moves along a B- field line into a region with a stronger B, the particle experiences a force that reduces the component of velocity parallel to the field. This force slows the motion along the field line and even reverses it ("**magnetic mirror**").

$$m \frac{dv_{\parallel}}{dt} = \frac{e}{m} E_{\parallel} - \mu \nabla_{\parallel} B \quad \leftarrow \text{Mirror force}$$

Magnetic moment (magnetic flux through the Larmor circle, **adiabatic invariant**)

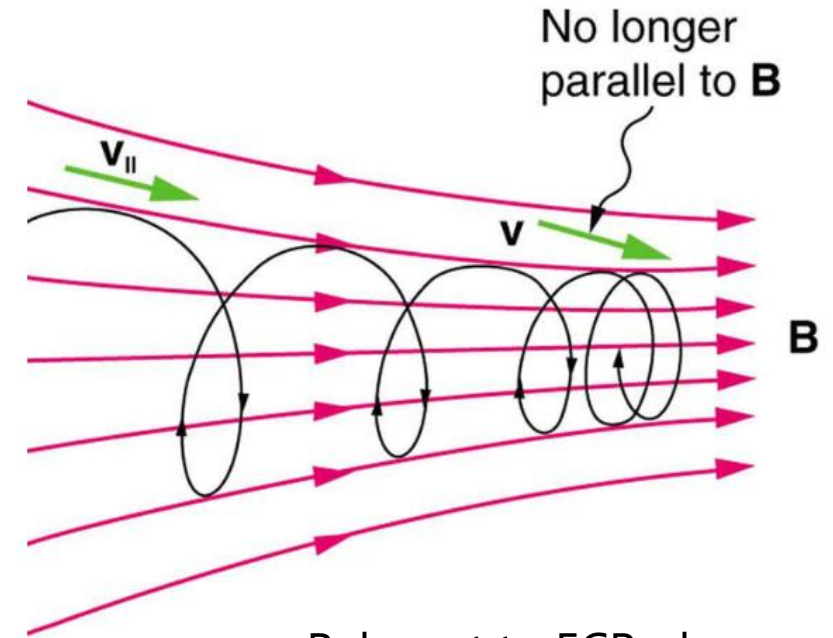
$$\frac{v_{\perp}^2}{B(z)} = \mu_0 = \text{const}$$

Energy conservation

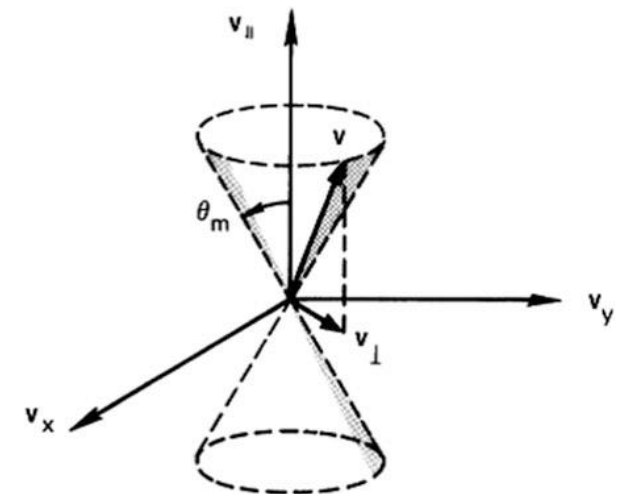
$$\frac{m}{2} (v_{\perp}^2 + v_{\parallel}^2) = \text{const}$$

Particles lying within the **loss cone** are not confined:

$$\sin^2 \theta_m = \frac{B_0}{B_{\max}}$$



Relevant to ECR plasma sources



Charged particle drift in crossed E and B fields ($\mathbf{E} \times \mathbf{B}$)

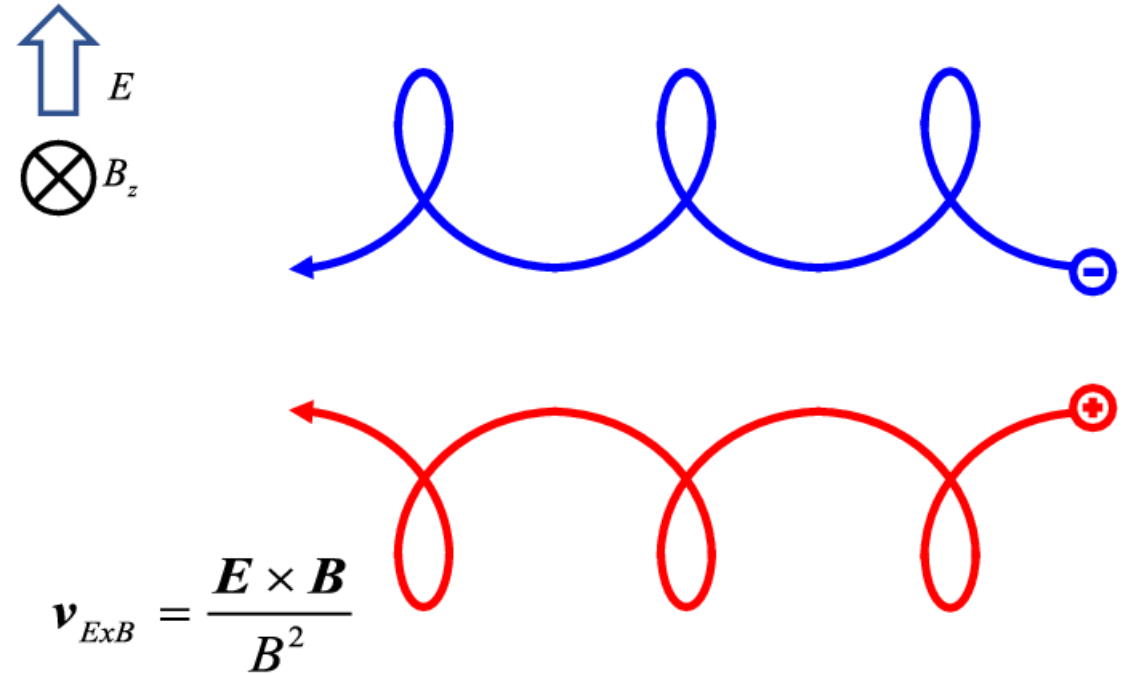
$$m \frac{d\mathbf{v}}{dt} = q(\mathbf{E} + \mathbf{v} \times \mathbf{B})$$

Particle motion in $\mathbf{E} \times \mathbf{B}$ fields is the sum of two motions: the usual circular Larmor gyration plus a drift of the **guiding center**.

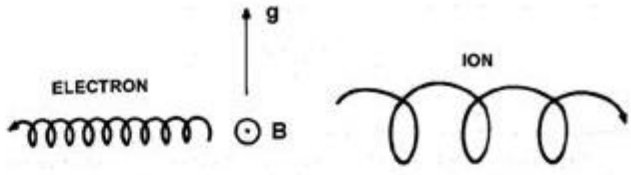
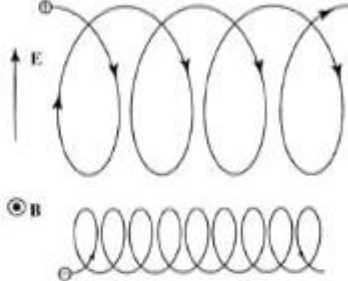
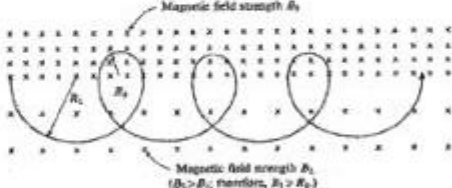
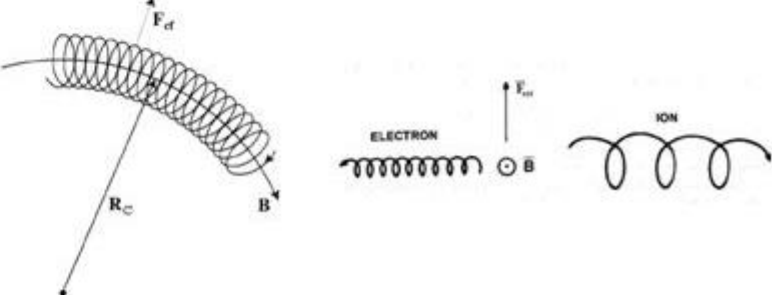
The magnitude of the drift velocity:

$$v_{E \times B} = \frac{E}{B}$$

The drift velocity direction and the magnitude do not depend on the particle charge and mass.

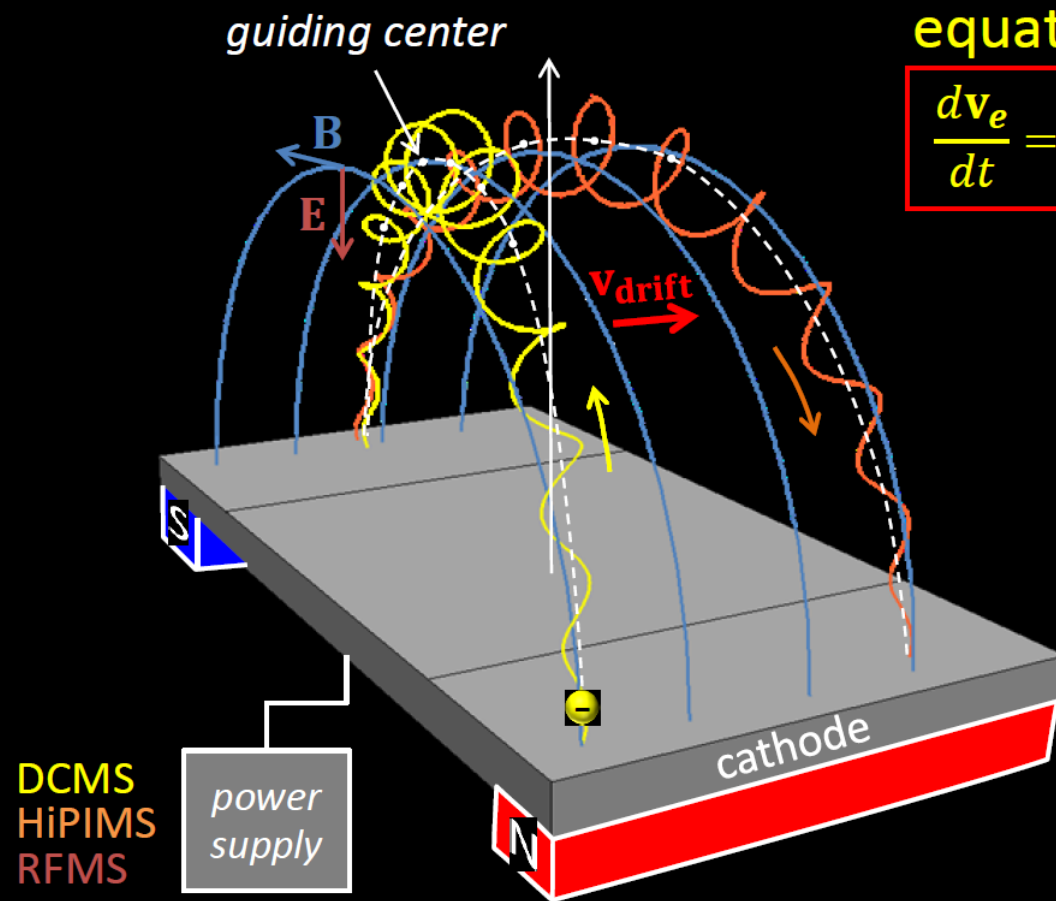


Summary of specific guiding center drifts

| | | |
|-------------------------------------------------------------------|----------------------------------------------------------------------------|--------------------------------------------------------------------------------------|
| <ul style="list-style-type: none"> Gravity: | $\bar{v}_g = \frac{m\bar{g} \times \bar{B}}{qB^2}$ |  |
| <ul style="list-style-type: none"> Electric Field: | $\bar{v}_E = \frac{\bar{E} \times \bar{B}}{B^2}$ |  |
| <ul style="list-style-type: none"> B-Gradient: | $\bar{v}_\nabla = \frac{mv_\perp^2 (\bar{B} \times \nabla B)}{2qB^3}$ |  |
| <ul style="list-style-type: none"> B-Curvature: | $\bar{v}_R = \frac{mv_\parallel^2 (\bar{R}_C \times \bar{B})}{qR_C^2 B^2}$ |  |

Motion of electrons in magnetron sputtering discharges

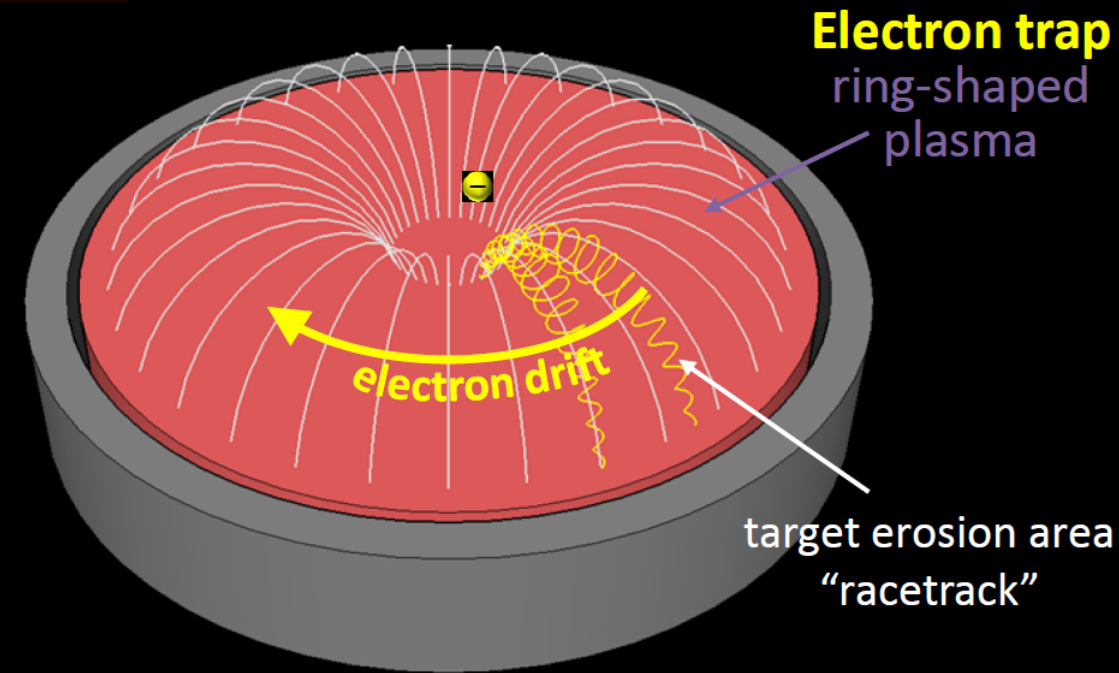
Motion of electron in crossed **electric** and **magnetic** field



equation of motion

$$\frac{d\mathbf{v}_e}{dt} = \frac{e}{m_e} (\mathbf{E} + \mathbf{v}_e \times \mathbf{B})$$

*Courtesy of Matjaž Panjan
Jožef Stefan Institute*



$\mathbf{E} \times \mathbf{B}$ drift

$$\mathbf{v}_{\mathbf{E} \times \mathbf{B}} = \frac{\mathbf{E} \times \mathbf{B}}{B^2}$$

∇B drift

$$\mathbf{v}_{\nabla B} = \frac{v_{\perp} r_L}{2} \frac{\nabla B \times \mathbf{B}}{B^2}$$

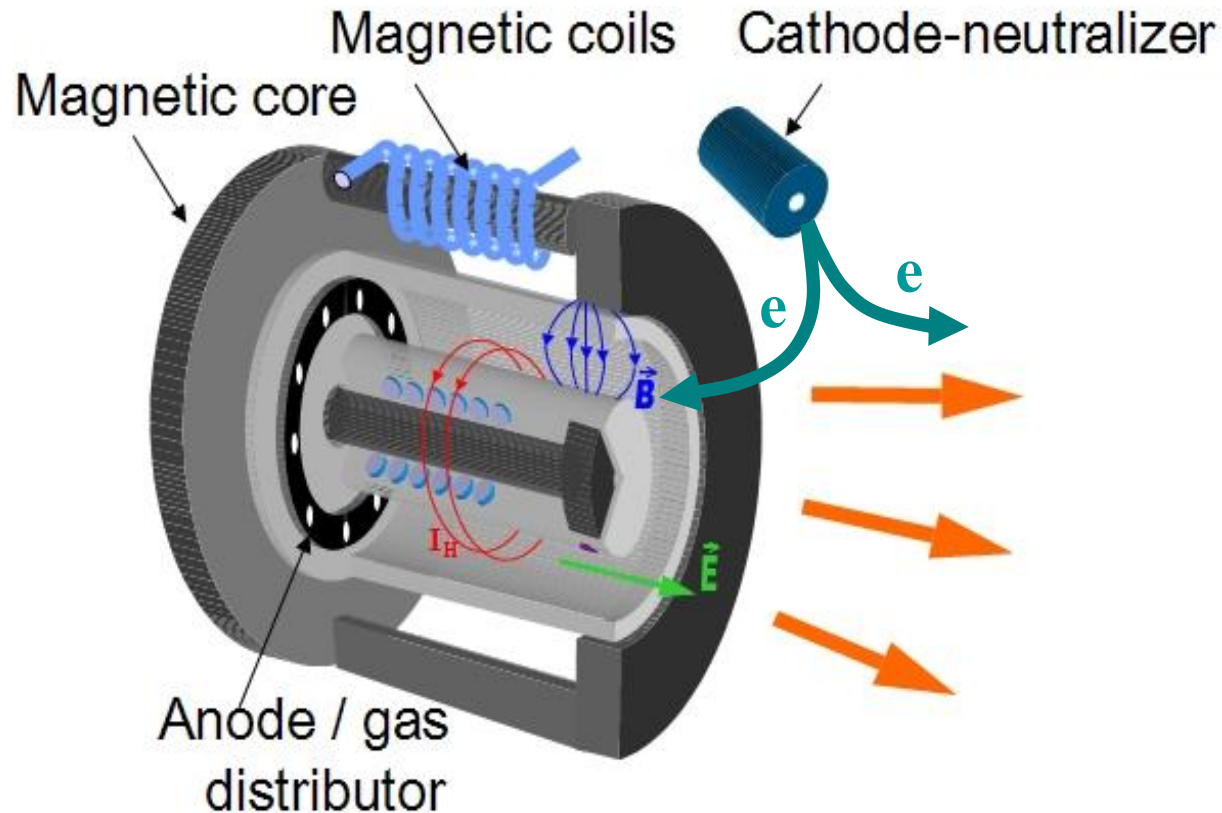
B-curvature drift

$$\mathbf{v}_R = \frac{m_e v_{\parallel}^2}{q} \frac{\mathbf{R}_C \times \mathbf{B}}{R_C^2 B^2}$$

Electron drift velocity

$$\mathbf{v}_{\text{drift}} = \mathbf{v}_{\mathbf{E} \times \mathbf{B}} + \mathbf{v}_{\nabla B} + \mathbf{v}_R$$

Hall current (anode layer) ion source = *Inverse Magnetron*



- Applied DC (stationary) fields: $\mathbf{E} \times \mathbf{B}$
- **Outward E-field** (in contrast to E in magnetrons)
- Quasineutral plasma: $n_e \approx n_i$
- Electrons $\mathbf{E} \times \mathbf{B}$ drift in azimuthal direction
- Heavier ions almost unaffected by B-field

$$r_{Li} > L \gg r_{Le} = \frac{m_e v_{\perp}}{eB}$$

- Equipotential magnetic field surfaces

$$\mathbf{E} = -\mathbf{V}_e \times \mathbf{B}$$

- Ions are accelerated by electric field
- Accelerated ion flux is neutralized by electrons

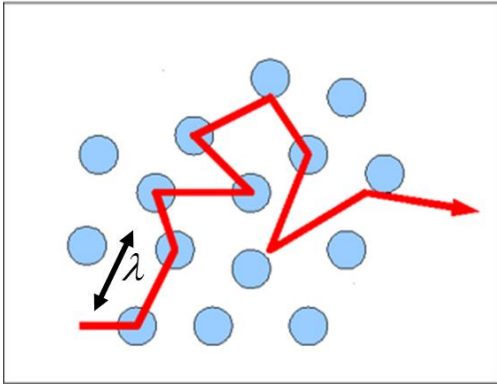
$$\Gamma_e = \Gamma_i = nv$$

Of all steady state laboratory magnetized plasmas, Hall current plasma can withstand the strongest DC E-field

| Device\Parameter | R cm | L cm | T eV | B Gauss | E_{\max} V/cm |
|---------------------------------------|------|------|--------|---------|-----------------|
| LAPD at UCLA | 50 | 1700 | 2-5 | 400 | 4-18 |
| Compact Auburn Torsatron | 17 | 53 | 10 | 1000 | 5 |
| Blaamann | 8 | 65 | 9 | 570 | 2-6 |
| Continuous Current Tokamak | 40 | 150 | 150 | 3000 | 120 |
| ALEXIS at Univ. Auburn | 10 | 170 | 5 | 100 | 2 |
| Reflex arc | 2.5 | 300 | 5 | 4000 | 20 |
| Mistral | 11.5 | 140 | 1.4 | 220 | |
| Maryland Centrifugal Experiment (MCX) | 27 | 250 | 3 | 2000 | |
| CSDX | 10 | 280 | 1.5-3 | 650 | 3-4 |
| WVU Q-machine | 4 | 300 | 0.2 | 1400 | 14 |
| Hall current plasma | 2 | 2 | 20-100 | 100-300 | 500-1000 |

Cross-field diffusion and transport – *fluid picture*

No magnetic field



$$0 = \underbrace{qn\mathbf{E}}_{\text{Electric field}} - \underbrace{T\nabla n}_{\text{Pressure}} - \underbrace{m\nu n\mathbf{V}}_{\text{Friction force}}$$

$$\mathbf{V} = \boxed{\frac{q}{m\nu}}\mathbf{E} - \boxed{\frac{T}{m\nu}}\frac{\nabla n}{n}$$

$$\mathbf{V} = \pm\mu_0\mathbf{E} - D_0\frac{\nabla n}{n}$$

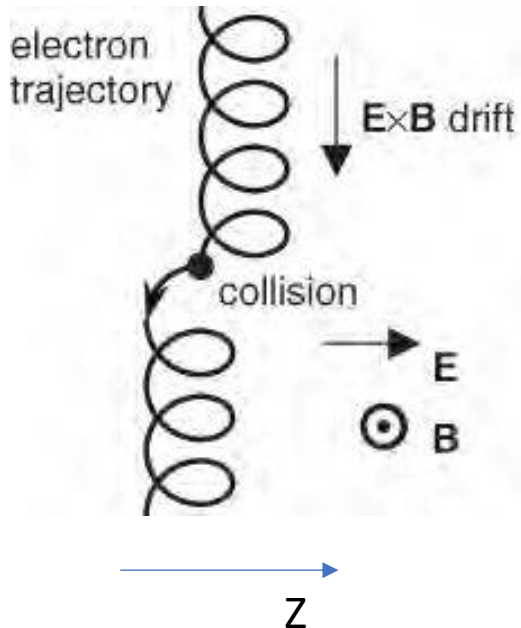
Diffusion (random walk)

$$D_0 = \frac{\lambda^2}{\tau} = \nu\lambda^2 = \frac{T}{m\nu}$$

$\lambda = 1/n\sigma$ - Mean free path

$\nu = n\langle v\sigma \rangle \propto P_g/kT_g$ - Collision frequency

In $\mathbf{E} \times \mathbf{B}$ fields



Any transport of charged particles across magnetic field requires a collision of the species either with the background gas or other scattering mechanisms (e.g. plasma fluctuations).

Diffusion and mobility across magnetic field $(\omega_{ec}/\nu)^2 \gg 1$ times smaller than that without magnetic field (and along B-field lines)

$$D_{\perp} \approx \nu_{ea} r_{Le} \approx \frac{D_0}{(\omega_{ec}/\nu_{ea})^2} \quad \mu_{\perp} \approx \frac{\mu_0}{(\omega_{ec}/\nu_{ea})^2}$$

Hall parameter

Short-circuit of magnetized plasma (Simon effect)

Simon short circuit: for $E \times B$ plasma in a chamber with conductive (equipotential) walls, global ambipolarity (**total losses of ions and electrons in quasineutral plasma are equal**) is maintained by the closure of plasma currents through the chamber walls.

$$\oint \Gamma_i \cdot d\mathbf{S} = \oint \Gamma_e \cdot d\mathbf{S}$$

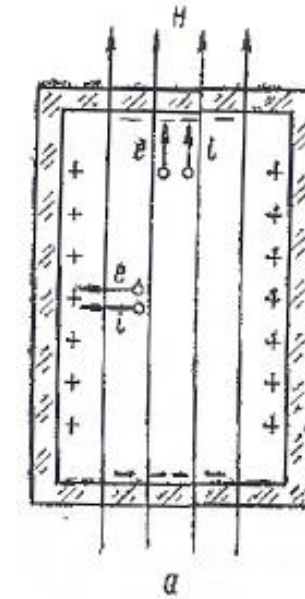
Flux of magnetized electrons across B-field:

$$\Gamma_{e\perp} = n_e v_{e\perp} = \mu_{e\perp} n_e E_x - D_{e\perp} \frac{\partial n}{\partial x}$$

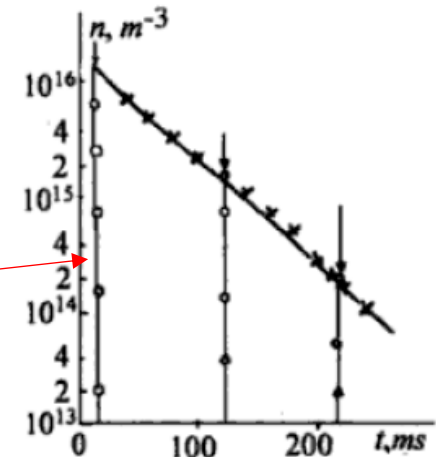
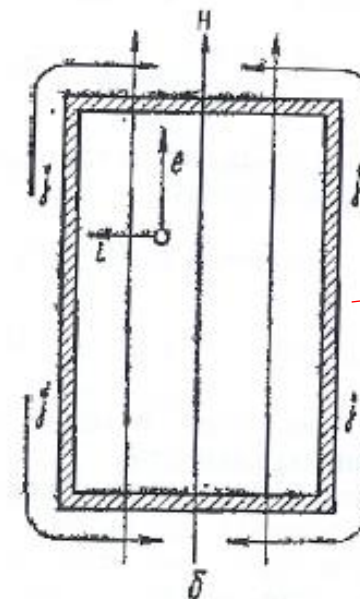
much smaller than the flux of heavier (often unmagnetized in LTP) ions: $\Gamma_{e\perp} \gg \Gamma_{i\perp}$

Along the B- field, electron flux dominates over ion flux: $\Gamma_{e\parallel} \gg \Gamma_{i\parallel}$

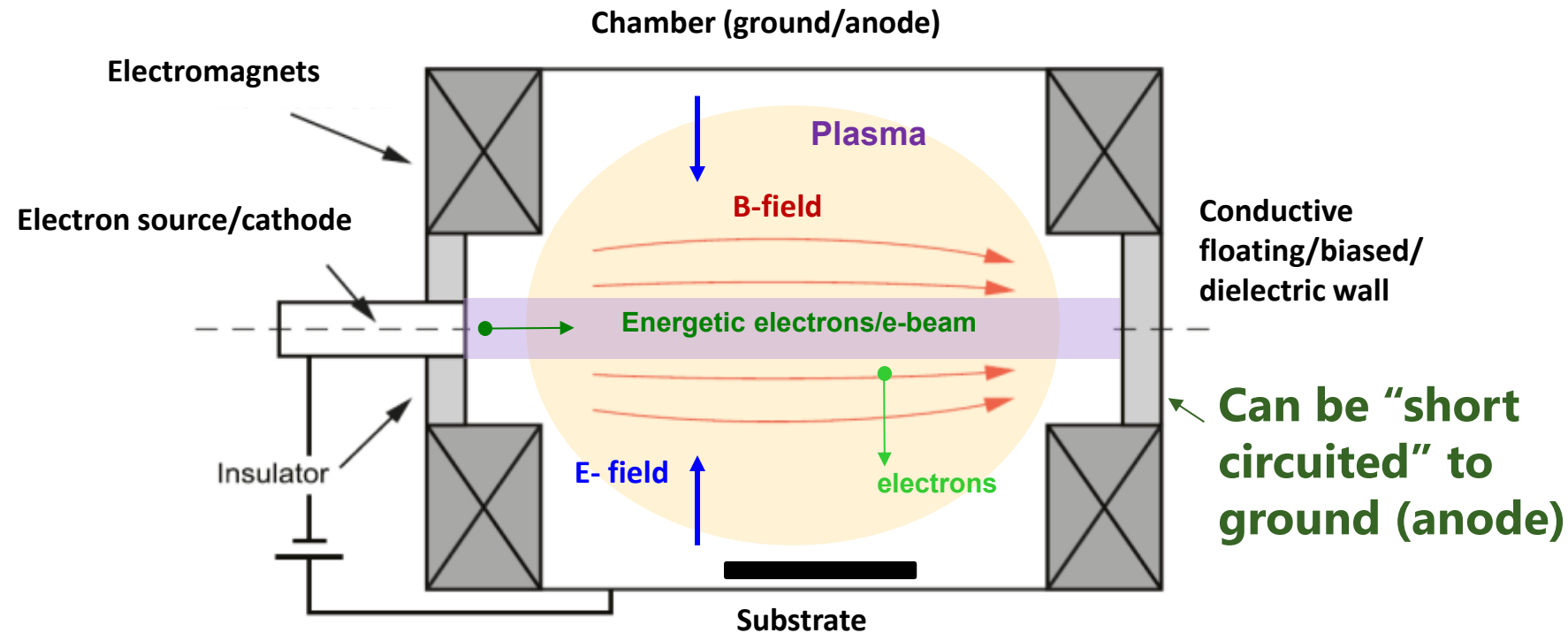
End & side walls disconnected



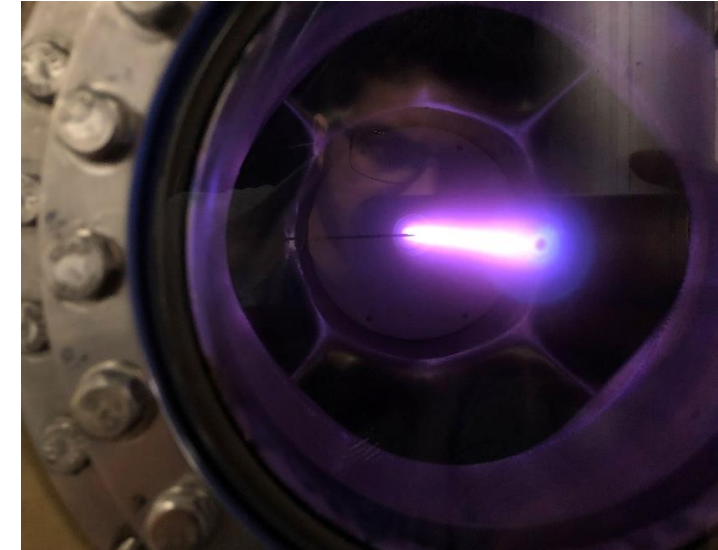
End & side walls connected



E×B plasma generated by electron beam



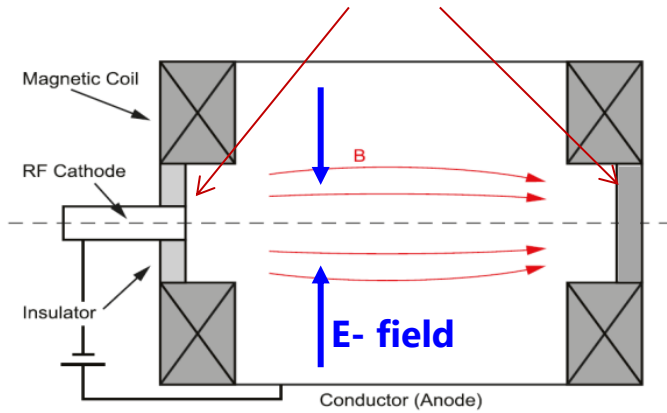
2 keV x 1 mA e- beam in Argon,
100 mtorr, B= 100 Gauss



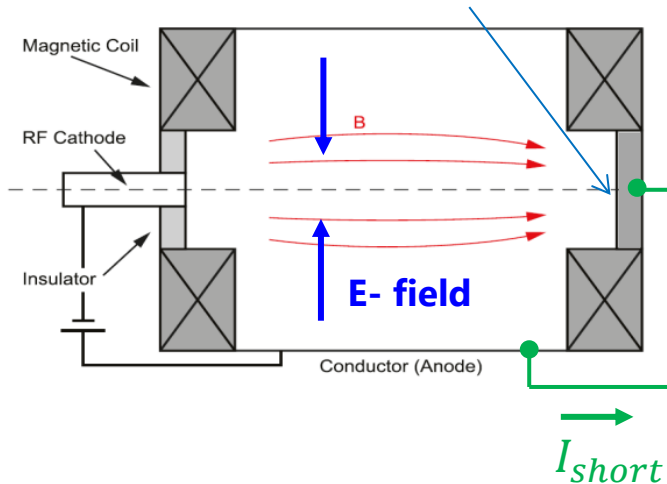
- **Applied voltage to extract electrons from the cathode and energize them**
 - E-beam/non-thermal electrons to generate plasma –energy control by “dialing” voltage
- **Applied magnetic field to confine and stratify plasma:**
 - Reduce the spread of electrons by collisions with neutral atoms, $\frac{\omega_{ce}}{\nu_{eb}} \gg 1$
 - Separate regions with energetic plasma (center) and cold plasma (vicinity)
 - Substrate placed at the periphery
- **Electric field – across magnetic field – to control fluxes to the substrate**

Example of a short-circuit effect in e-beam $E \times B$ plasma

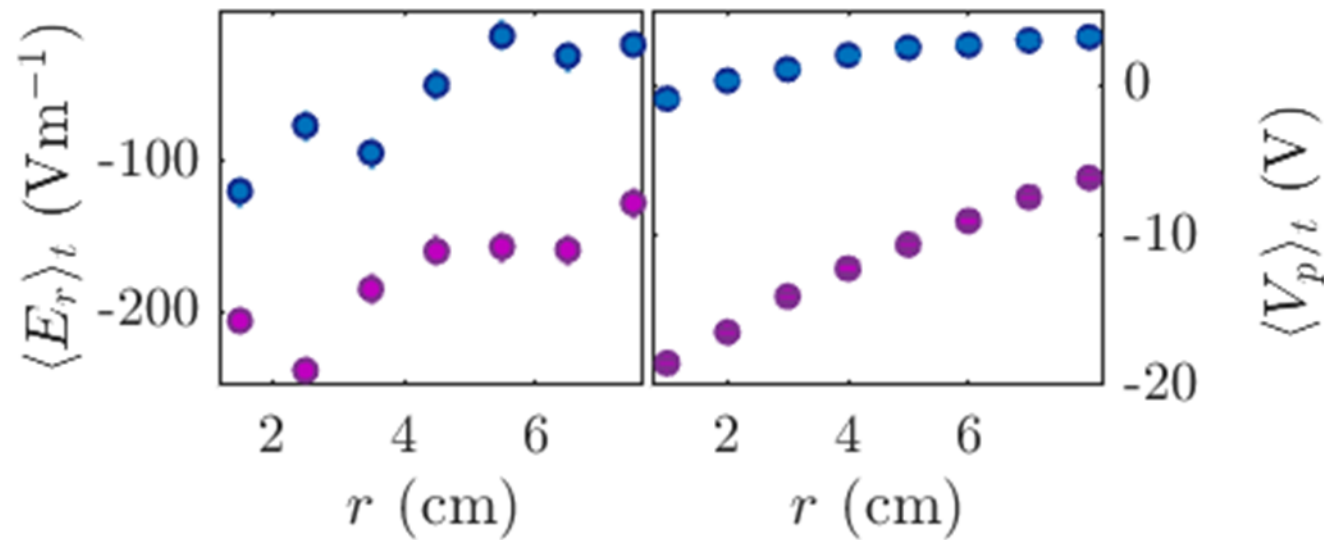
Ceramic end walls



Metallic end wall

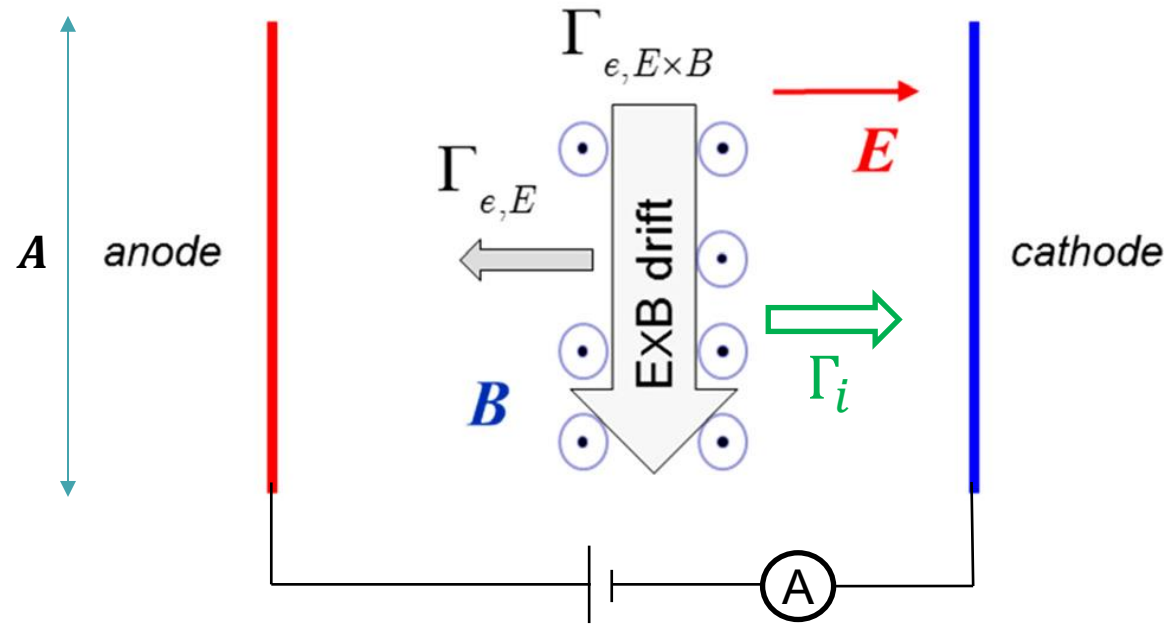


Time-averaged plasma potential distributions measured with an electrostatic probes



With conductive boundaries at the same potential, the electric field in plasma is greatly reduced due to wall conductivity (short-circuit effect).

Cross-field current in $E \times B$ plasma devices



Currents between electrodes:

$$I_d = q\Gamma A = e\Gamma_{e\perp}A + e\Gamma_{i\perp}A$$

$$\Gamma_{e\perp} = \boxed{\mu_{e\perp}} n_e \left[E - (1/en_e) \frac{d(n_e T_e)}{dz} \right]$$

$$\Gamma_{i\perp} = n_i v_i$$

In experiments, we can measure all parameters to get **electron cross-field mobility**:

- discharge current I_d in the **electrical circuitry**
- plasma density, $n_e \approx n_i$, electron temperature, T_e , by **Langmuir probes** (*Godyak's lecture*) or laser **Thomson scattering**
- ion velocity, v_i , by **Laser-Induced Fluorescence** (LIF) (*Donnelly's lecture*)
- Electric field, E , by electrostatic probes (potential profile) or deduce from LIF

Anomalous enhanced electron cross-field transport

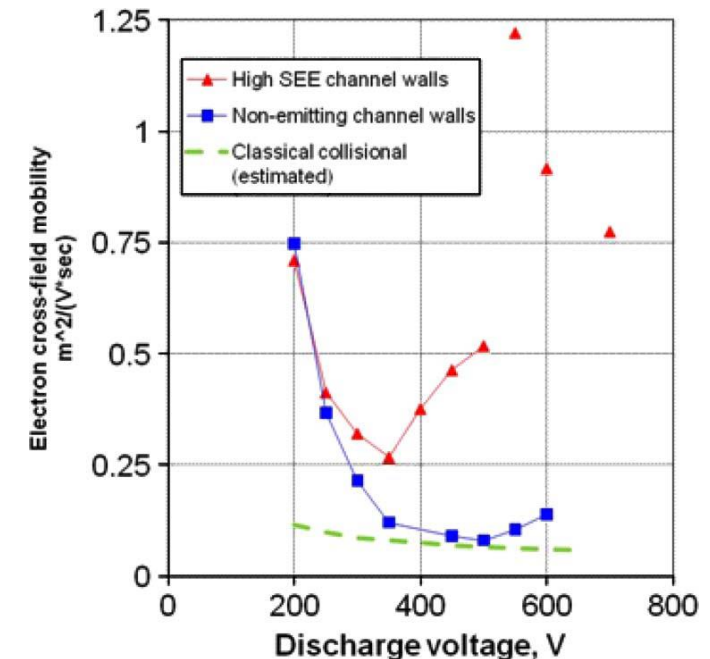
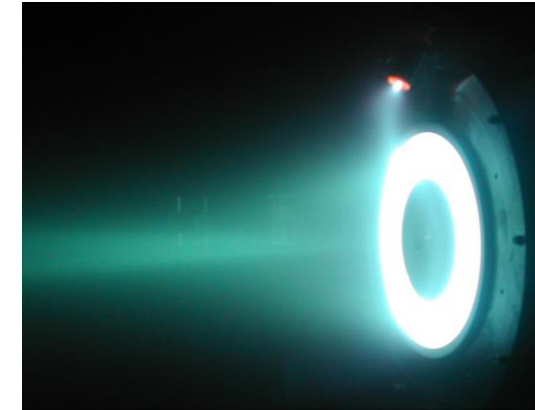
The figure shows mobility measurements at the location of the maximum E-field, for a Hall thruster (ExB plasma source similar to the anode layer ion source).

We clearly see that the experimental electron cross-field mobility is much larger than the classical (collisional) electron mobility.

This confirms that mechanisms other than electron-atom collisions must contribute to cross-field electron transport in a large part of the ExB plasma.

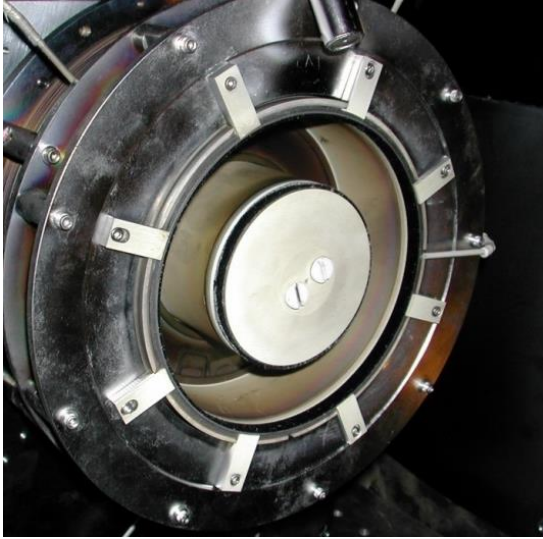
This situation is typical to many $E \times B$ plasma sources, especially operating at low pressures (≤ 1 mtorr)

12 cm diameter, 1 kW, Xenon Hall thruster

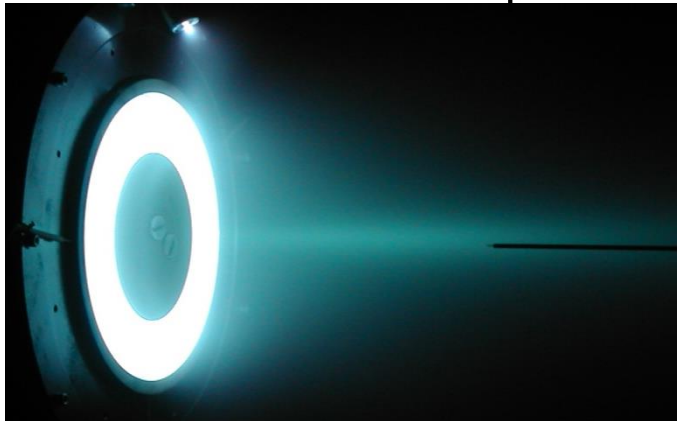


What are possible causes of this anomaly?

12 cm diameter, 2kW Hall thruster



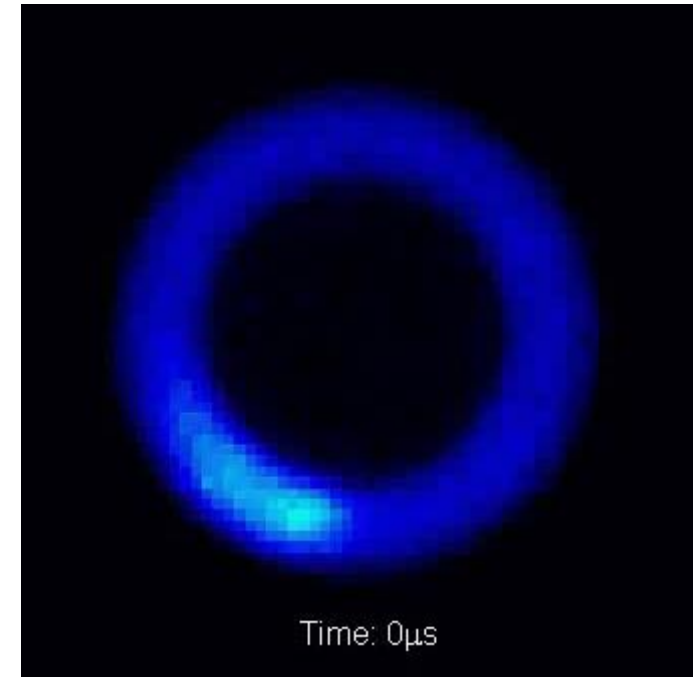
Xenon operation



Plasma non-uniformity

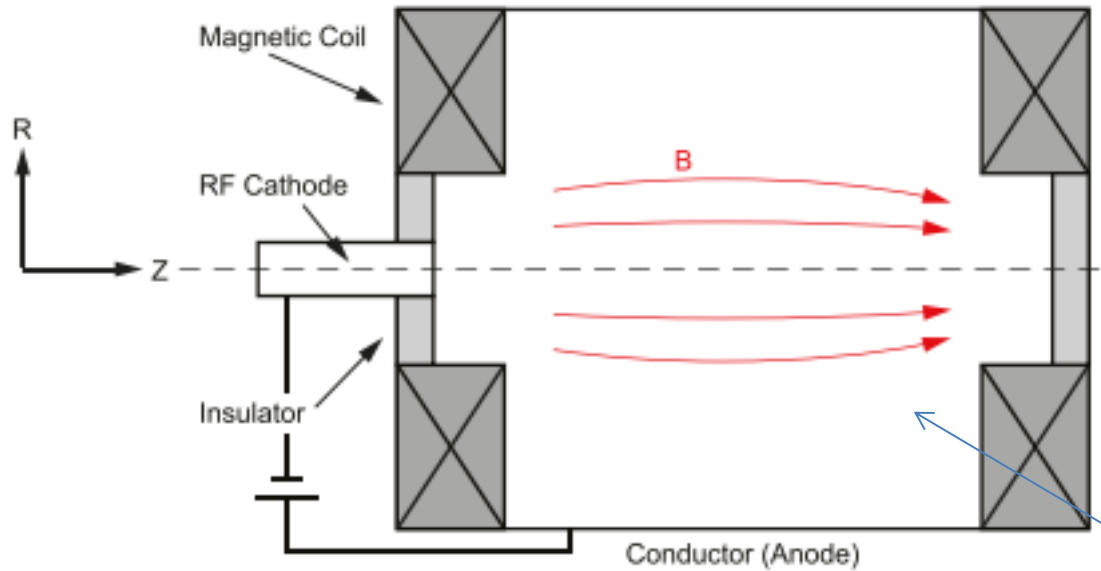
Current conducting ExB rotating “spoke”

Fast frame imaging 60 kfps



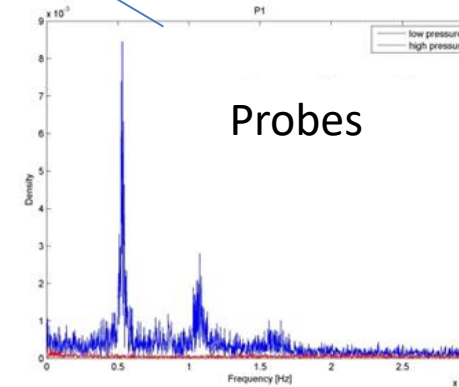
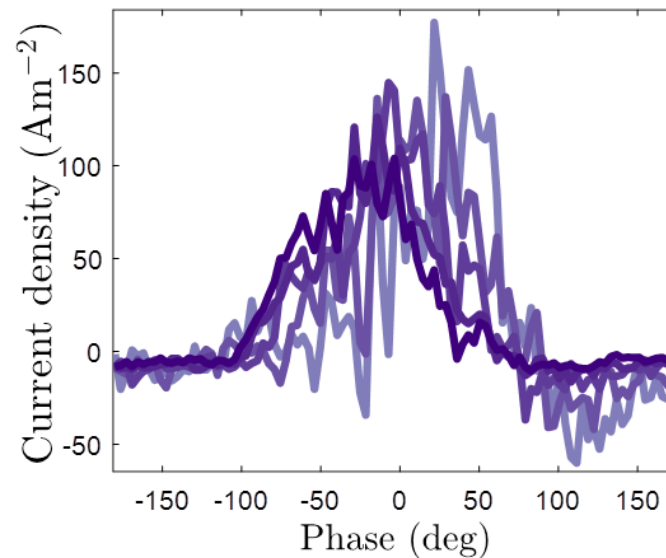
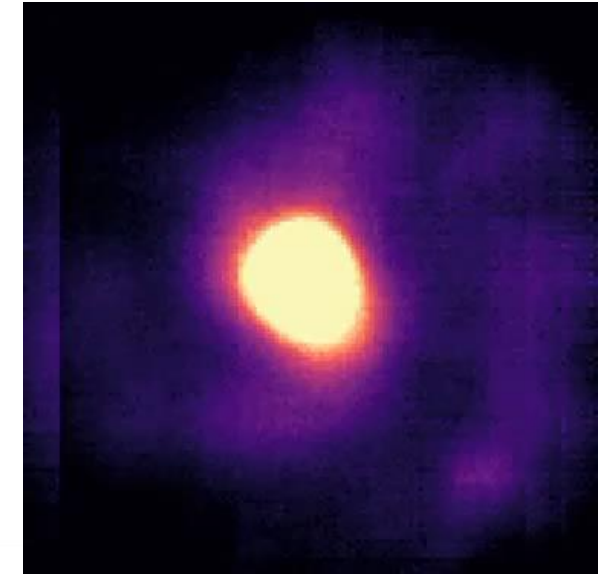
- Spoke frequency ~ 10 kHz
- 10's times slower than E/B
- **Conduct > 50-70% of the discharge current**

$E \times B$ rotating spoke in e-beam generated $E \times B$ plasma



FFI

Experiment, Xenon, 0.1 mtorr



5 kHz

Skoutnev et al., *Rev. Sci. Instrum.* **89** (2018)

Rodriguez et al., *Phys. Plasmas* 26, (2019)

Almost 100% of the electron current across the magnetic field through the spoke

Plasma self-organization in magnetron sputtering discharges

continuous voltage



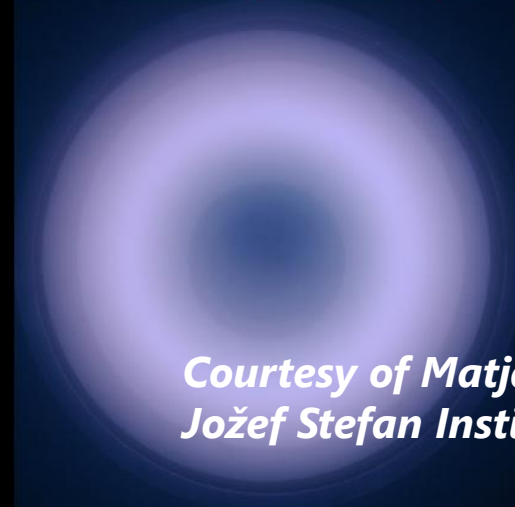
DCMS

pulsed voltage



HiPIMS

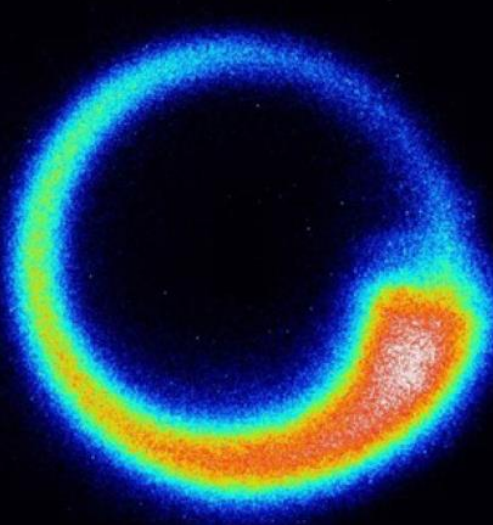
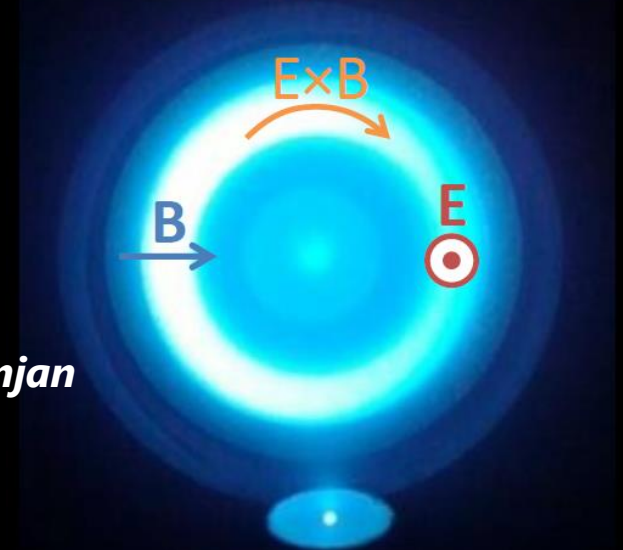
oscillatory voltage



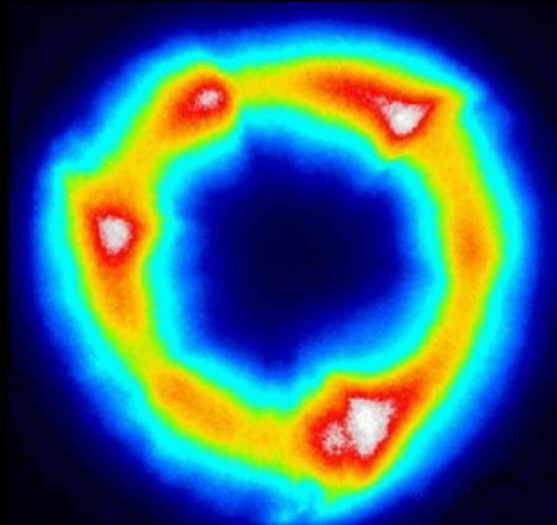
*Courtesy of Matjaž Panjan
Jožef Stefan Institute*

RFMS

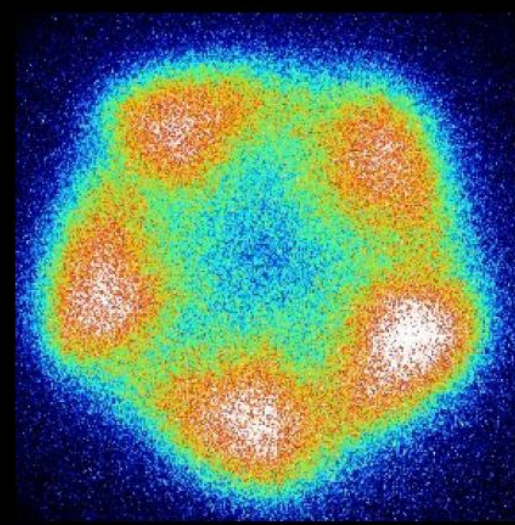
Hall thrusters



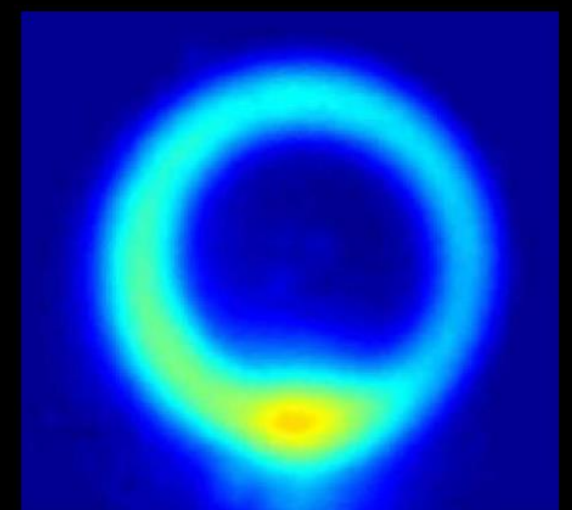
*M. Panjan et al Plasma Sources
Sci Technol 24 065010 (2015)*



*M. Panjan Plasma Sources
Sci Technol 33 055015 (2024)*



*M. Panjan J App Phys
125 20 (2019)*

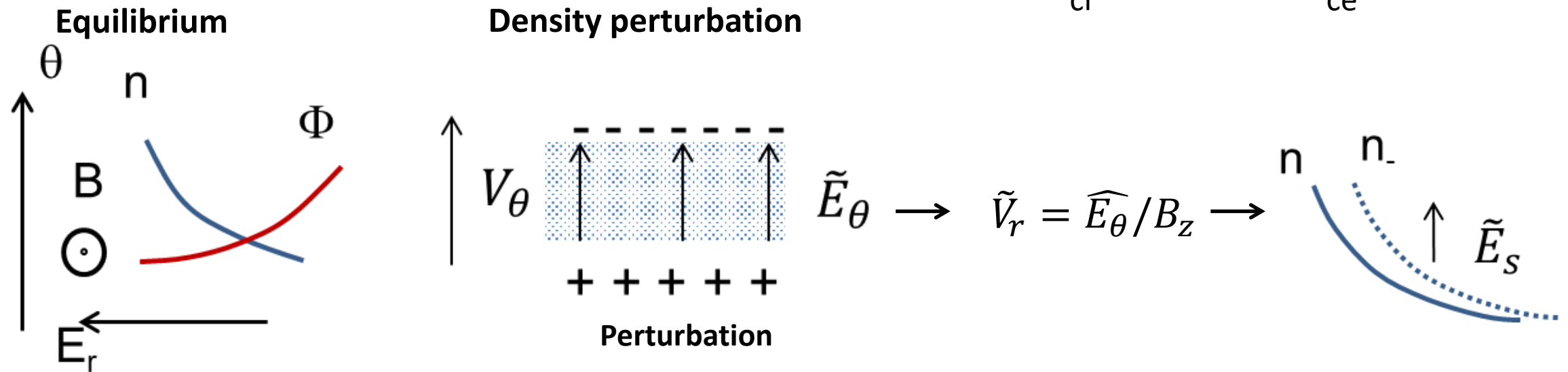


*C. Ellison, Y. Raitses, N. Fisch, IEEE
Transactions on Plasma Science,, 39 (2011)*

From theory, a key spoke mechanism: *gradient drift instability*

Collisionless Simon-Hoh instability: $\nabla n_{e0} \neq 0$ and $\nabla n_{e0} \cdot \mathbf{E}_{r0} > 0$

$$\omega_{ci} \ll \omega \ll \omega_{ce}$$

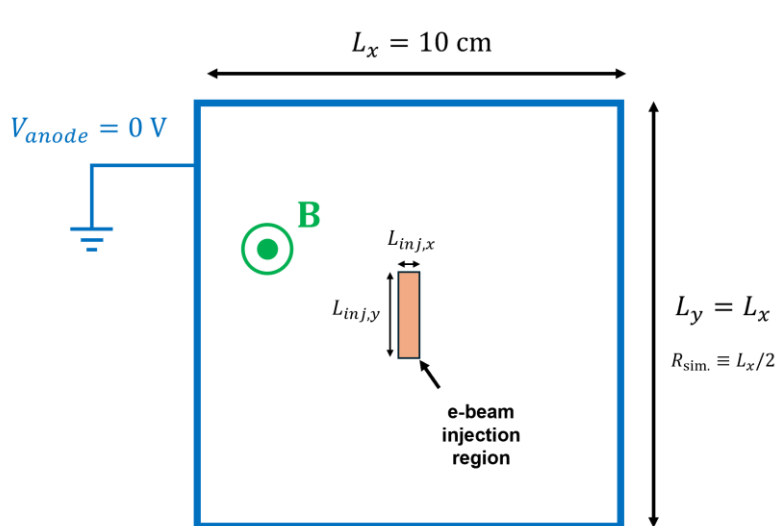


- Instability growth rate $\gamma \propto kc_s \sqrt{\frac{L_n}{L_E}}$
- Heating of electrons in the spoke may enhance ionization

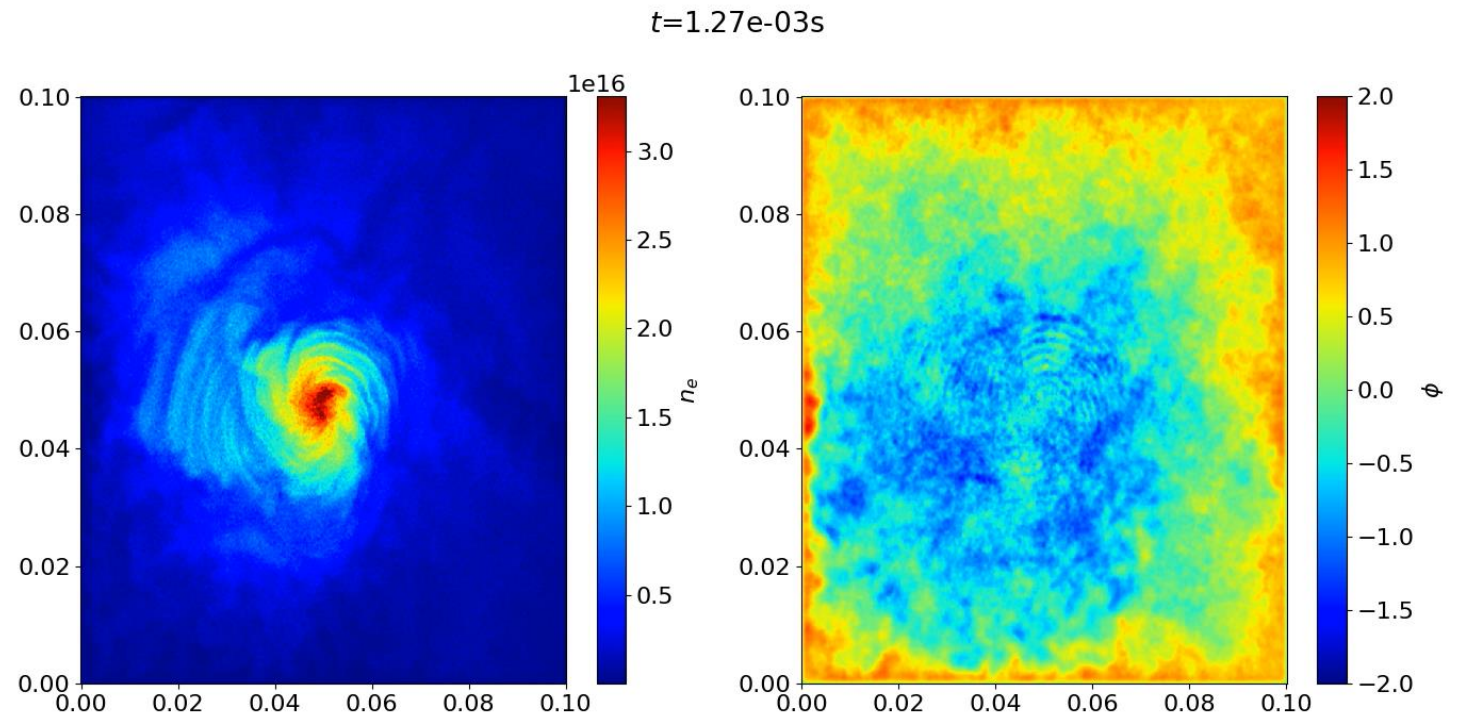
Extensive numerical investigations of $E \times B$ plasma

Power of Particle-in-Cell (PIC) simulations (*Kaganovich's lecture*)

PIC captured a complex $E \times B$ plasma dynamics measured in experiments and seem to confirm predicted mechanisms of the plasma structures including rotating spoke



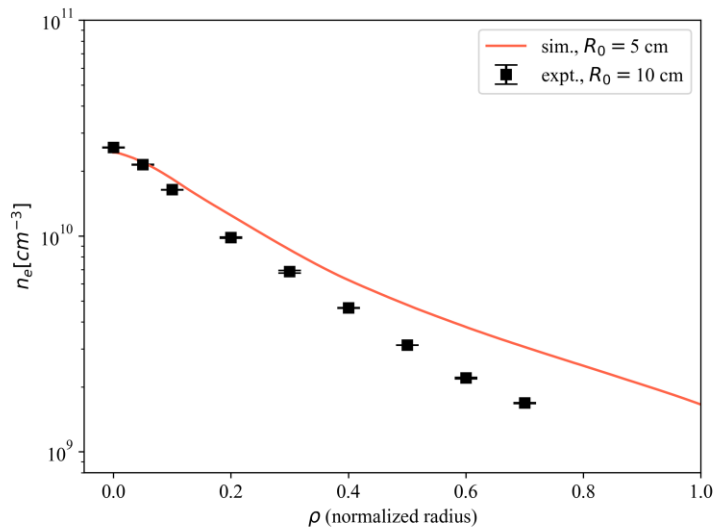
M. Tyushev et al., Phys. Plasmas **32** (2025)



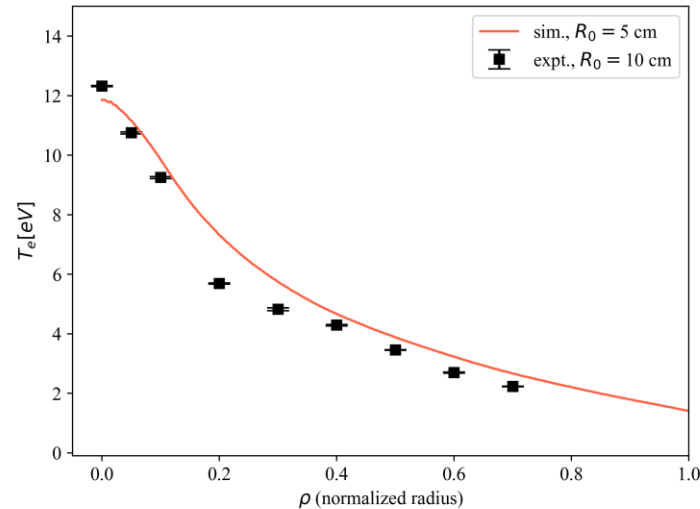
Comparison with experiments

- PIC is a very powerful computational method of plasma research, validated by experiments and capable to predict experiments.
 - Important for predicted designs of realistic plasma reactors/devices

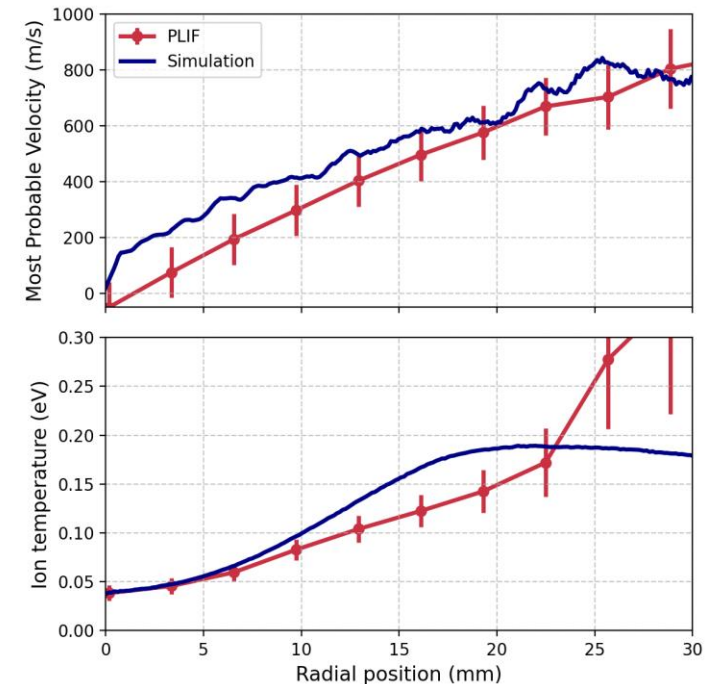
Plasma density by probe & PIC



Electron temperature by probe & PIC

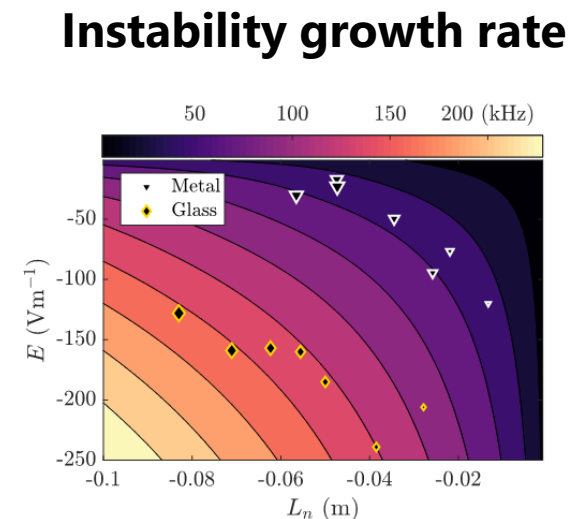
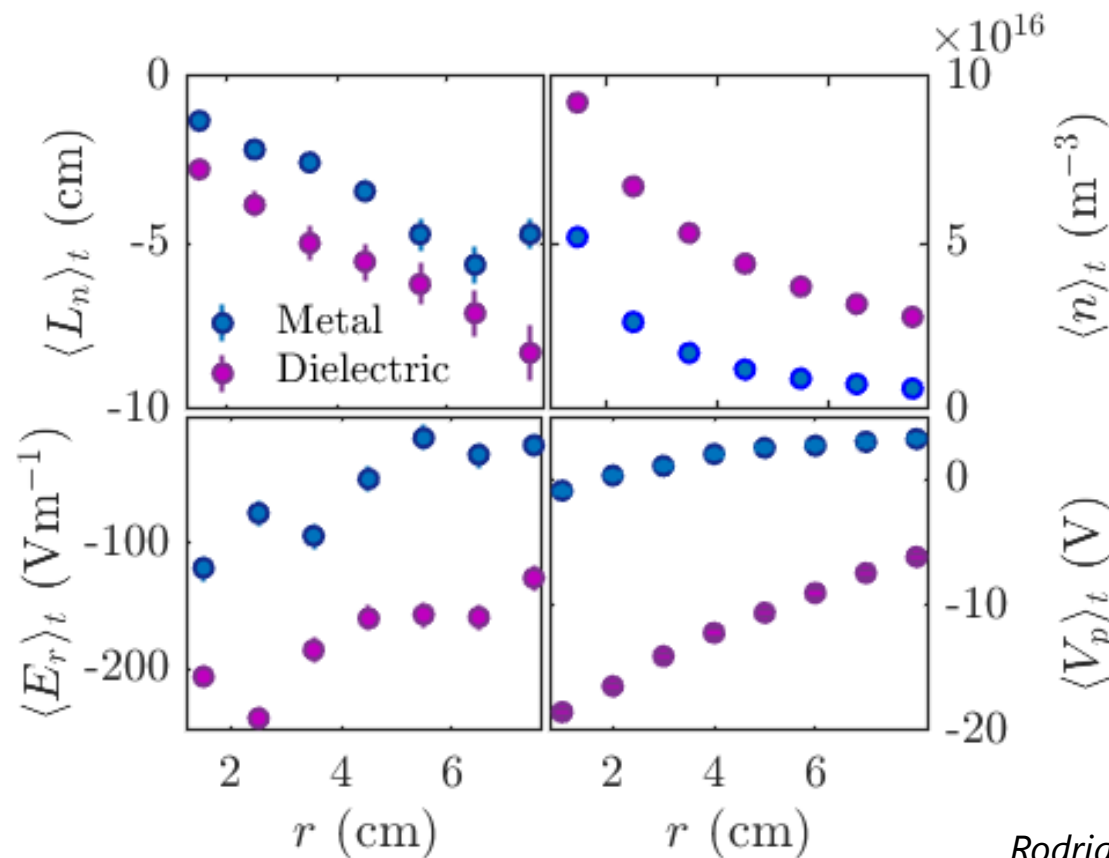
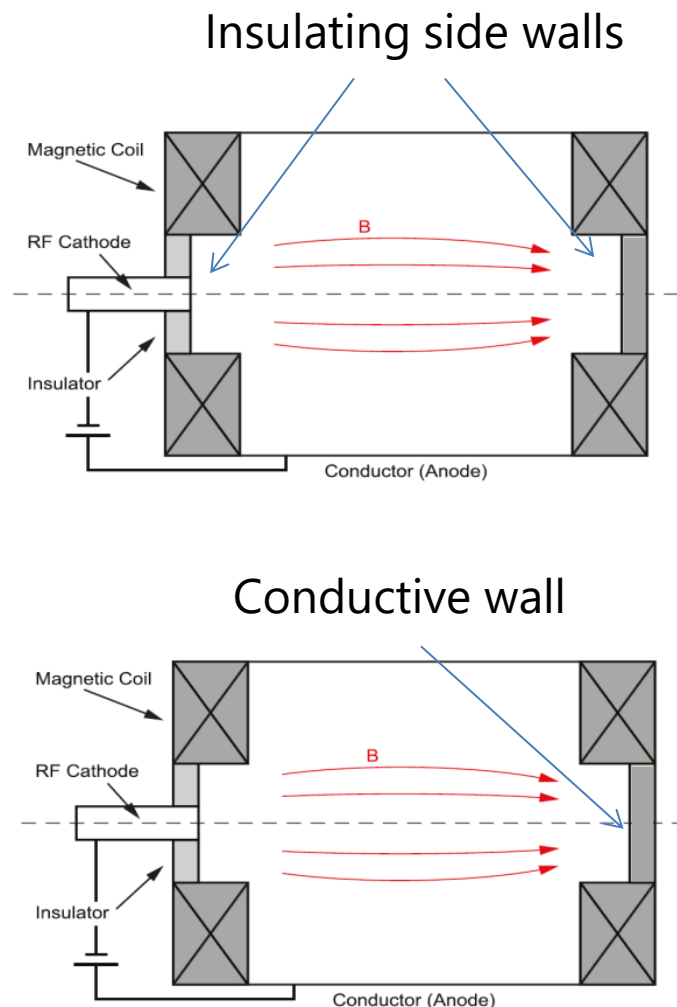


Ion velocity by LIF & PIC



Short-circuit effect to control $E \times B$ plasma

- Measured time-averaged plasma properties

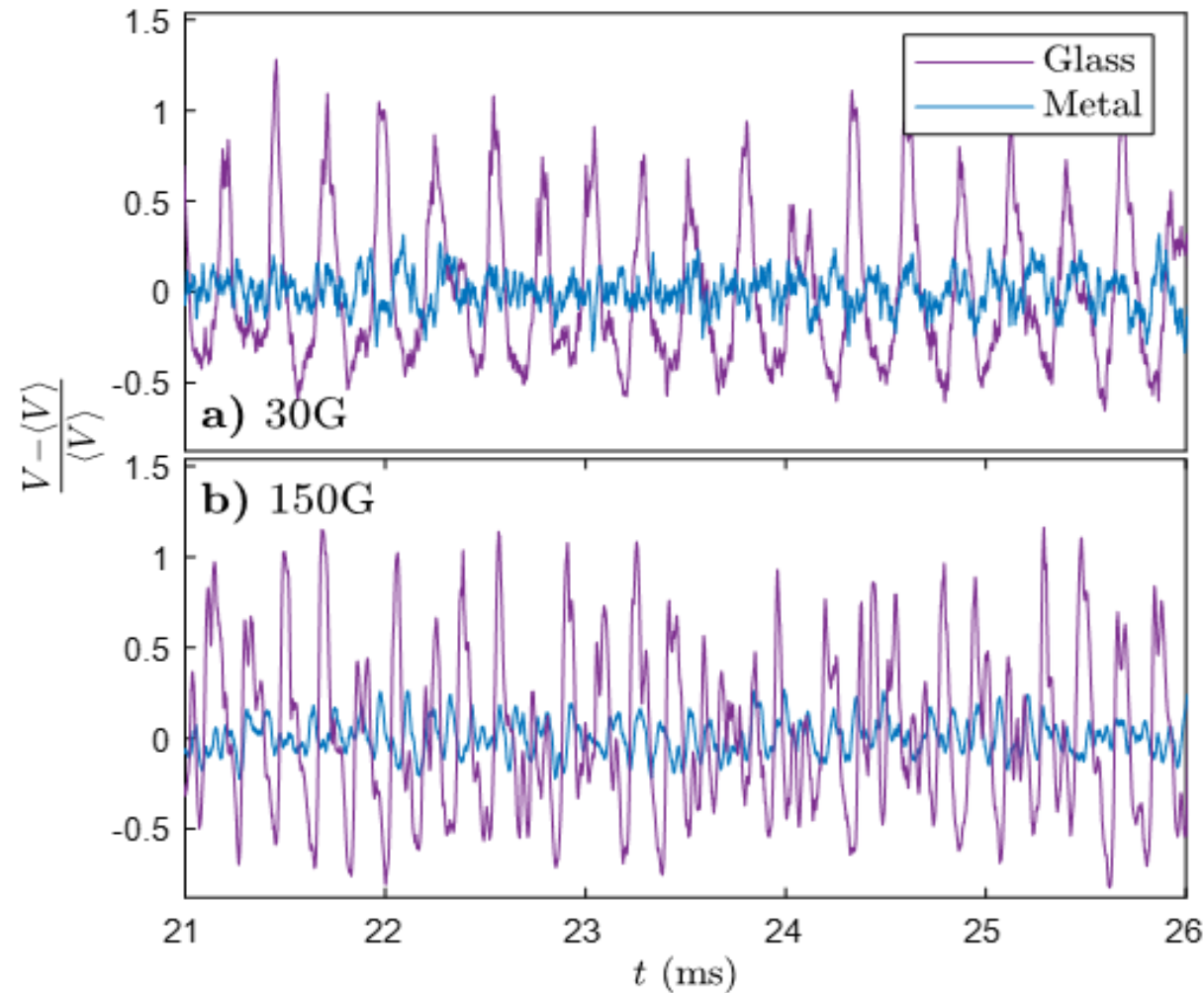


Rodriguez et al., Phys. Plasmas **26** (2019)

With conductive boundaries the electric field is greatly reduced.

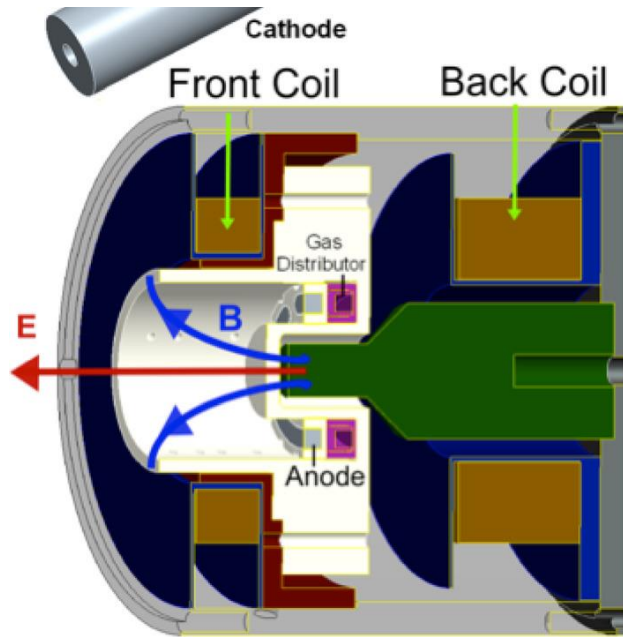
Suppression of spoke oscillations by short-circuit

- Oscillations of the plasma density

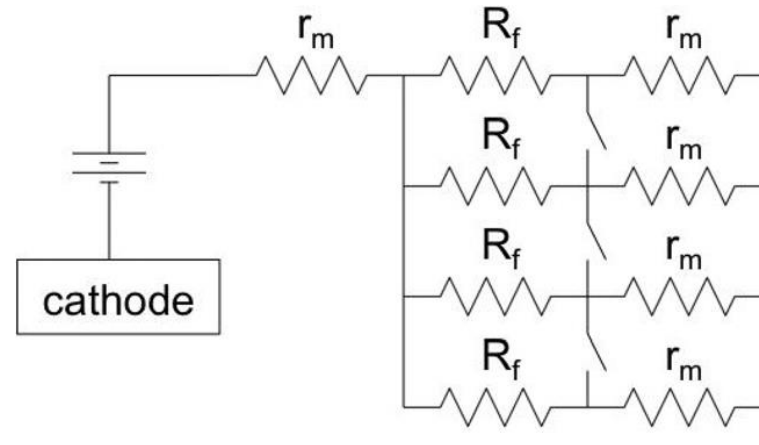


Spoke suppression by a feedback control

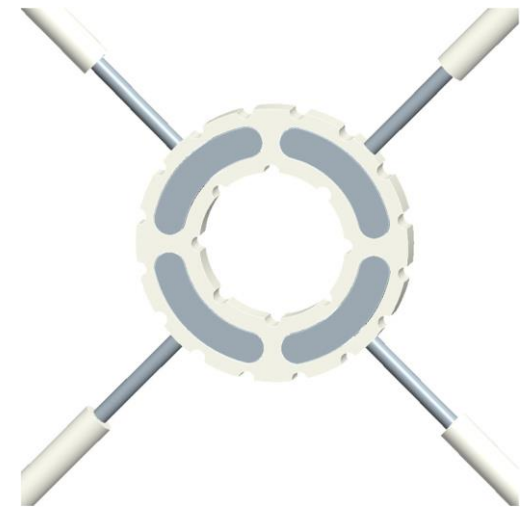
cylindrical Hall thruster (CHT)



- Segmented anode
- Resistors attached between each anode segment and the power supply



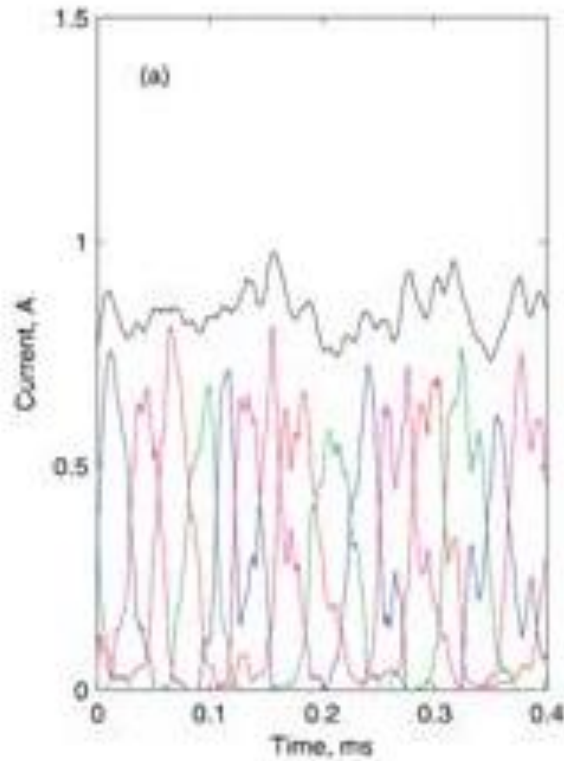
Anode
Segments



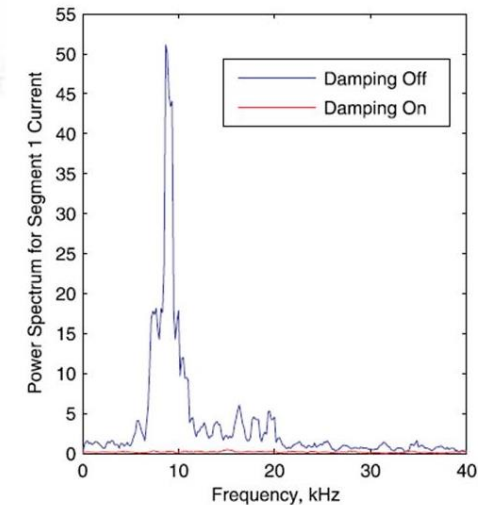
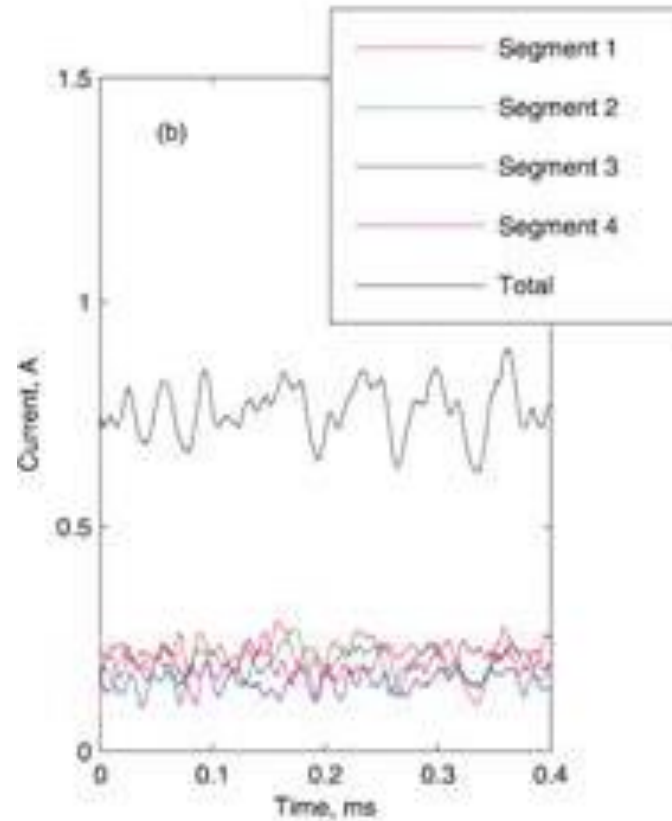
- Spoke increases the current through the segment leading to the increase the voltage drop across the resistor attached the segment.
- This results in the reduction of the voltage between the segment voltage and the cathode.

Feedback control results: mitigated spoke oscillations

- Feedback off

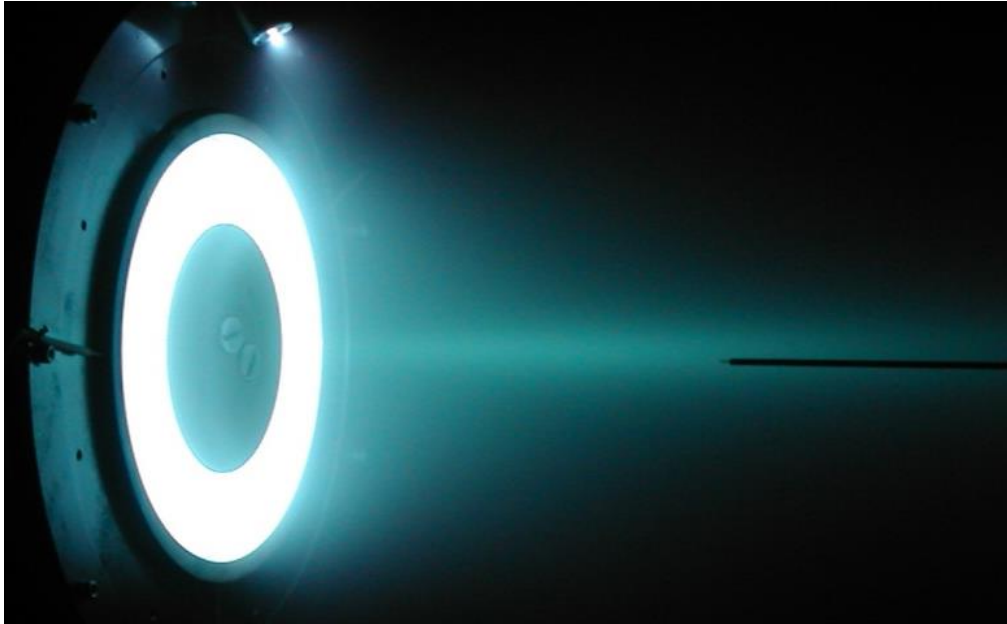


- Feedback on

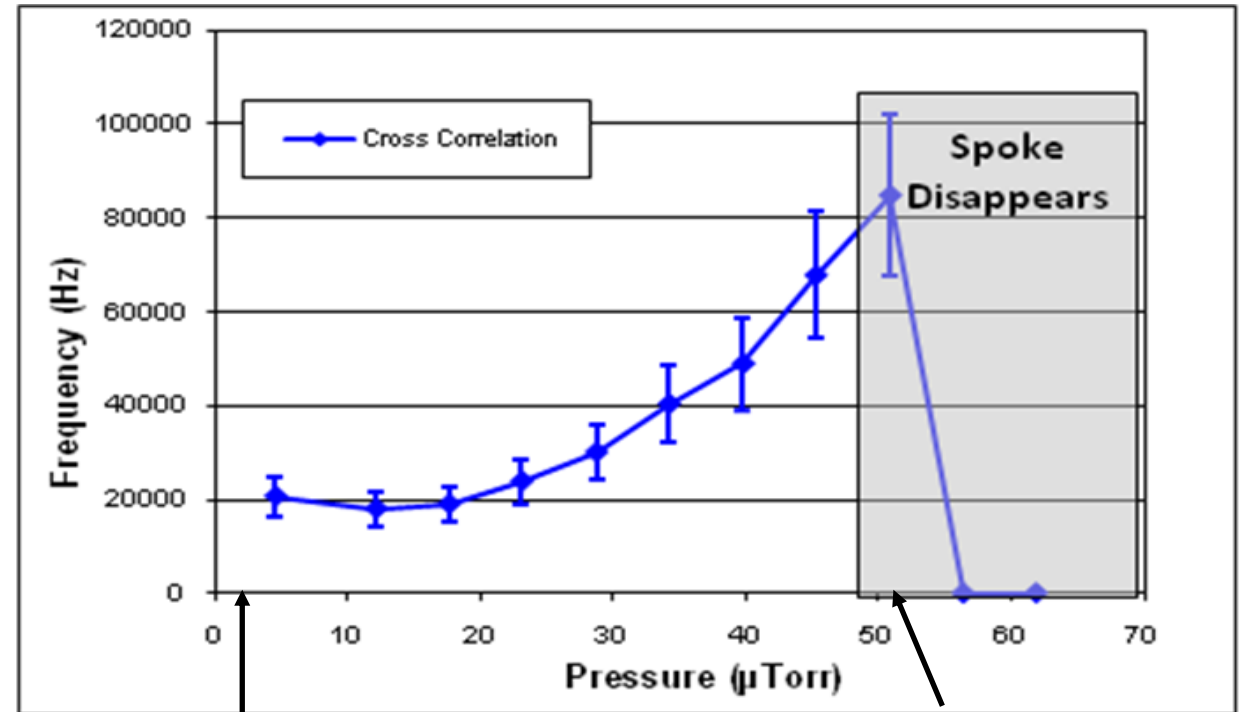


$E \times B$ instabilities in LTP may disappear at elevated pressures

- Xenon Hall thruster



- Cross-correlation from fast imaging



$\nu_{en} \sim 10^5 s^{-1}$

$\nu_{anom} \sim 10^8 s^{-1}$

$\nu_{en} \sim 10^6 s^{-1}$

Plasma structures like spoke are not always unwanted

In high-power impulse magnetron sputtering (HiPIMS), the discharge current during a pulse exceeds the time-averaged current by several orders of magnitude.

The pulses are typically 10–100 μs long and are repeated with a frequency of 10–1000 Hz. Such pulsing leads to the formation of dense plasma with a high degree of ionized sputtered species.

Key advantage of HiPIMS over conventional sputtering magnetrons (DC and RF) - high density of deposited films by HiPIMS.

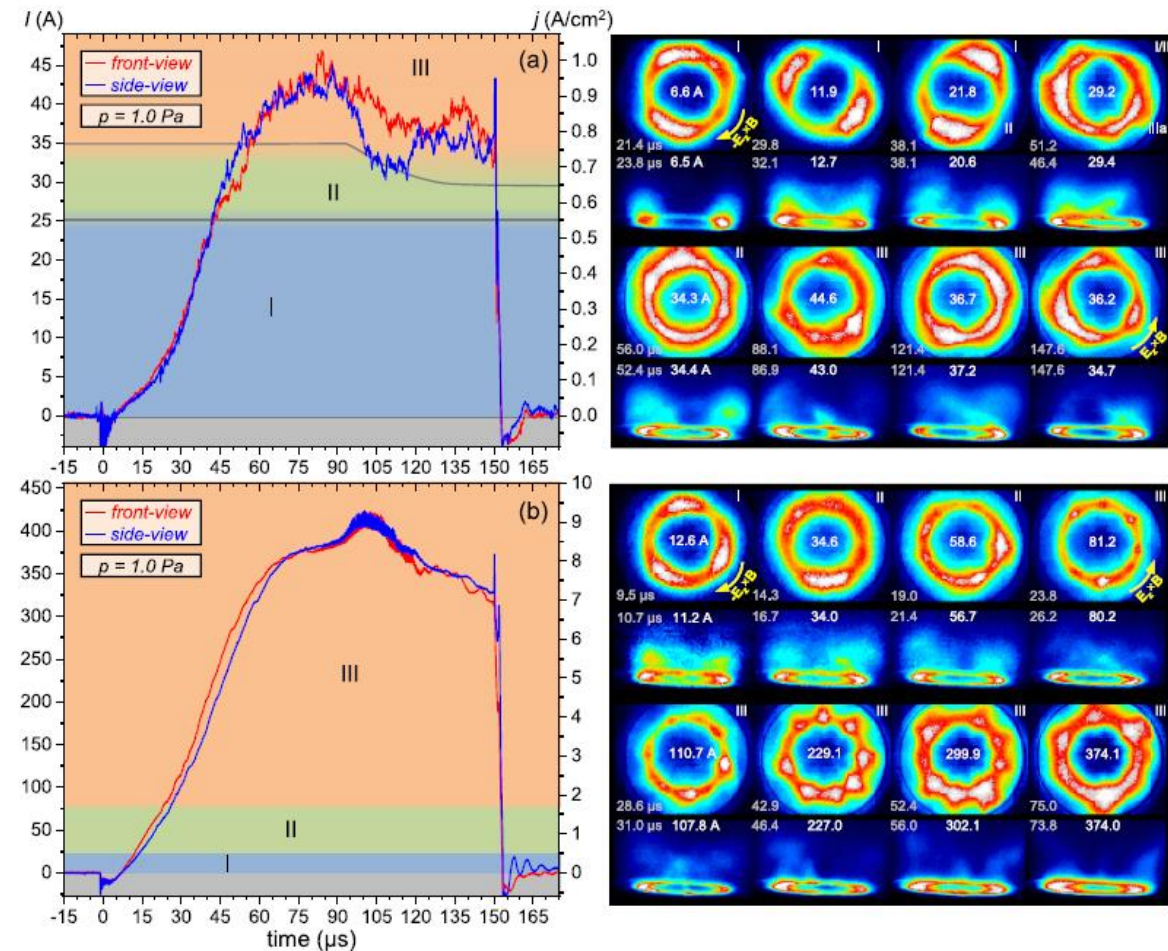
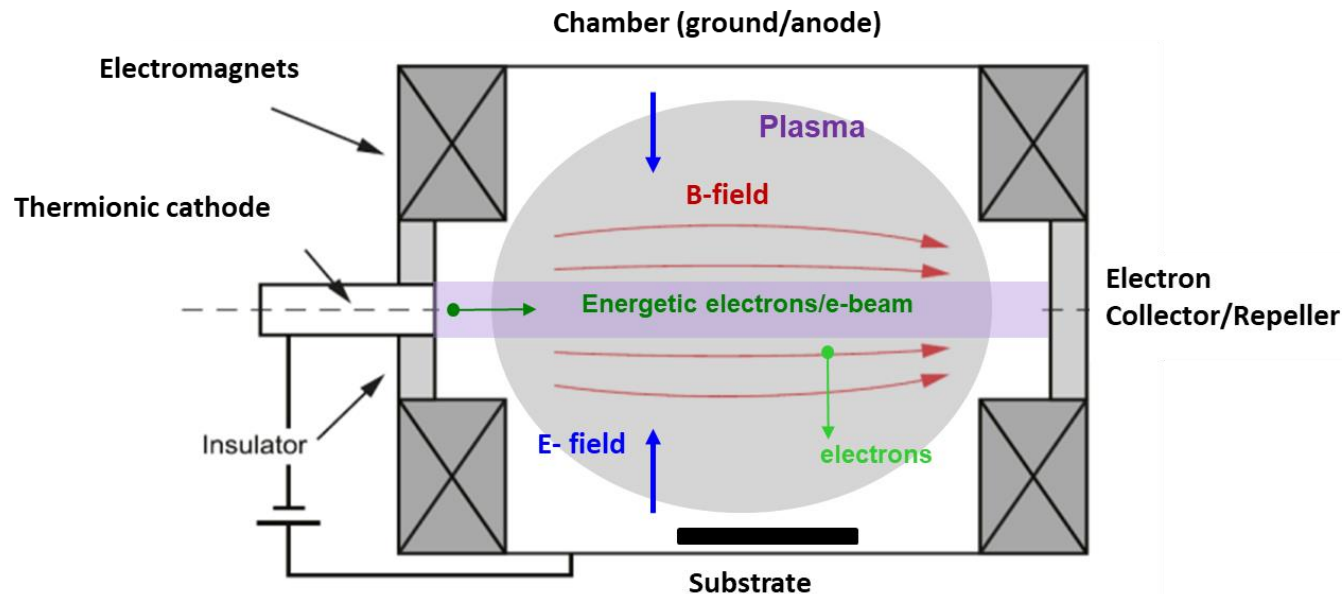


Figure 11. Current waveforms and typical plasma patterns from the front- and side-view perspective for three characteristic stages during a HiPIMS pulse. Plasma self-organization is shown for discharges operated at (a) $I_p = 40 \text{ A}$ and (b) $I_p = 400 \text{ A}$. Spokes in stage I typically display an elongated arrowhead-like shape and rotate in the $-\mathbf{E}_z \times \mathbf{B}$ direction, whereas in stage III spokes are shorter, exhibit a triangular shape, and rotate in the $\mathbf{E}_z \times \mathbf{B}$ direction. Spoke patterns in stage I and III are periodic or semi-periodic. In stage II spoke patterns and motion are highly irregular. The borders between the stages are approximate and specific to the Al target. Figures for other pressures can be found in supplementary materials V15 and V16.

**Gentle processing of (ion-sensitive) sensitive materials
is a motivation for new $E \times B$ (and not only) plasma
sources for *microelectronics and QIS***

Why electron-beam generated E×B plasma?

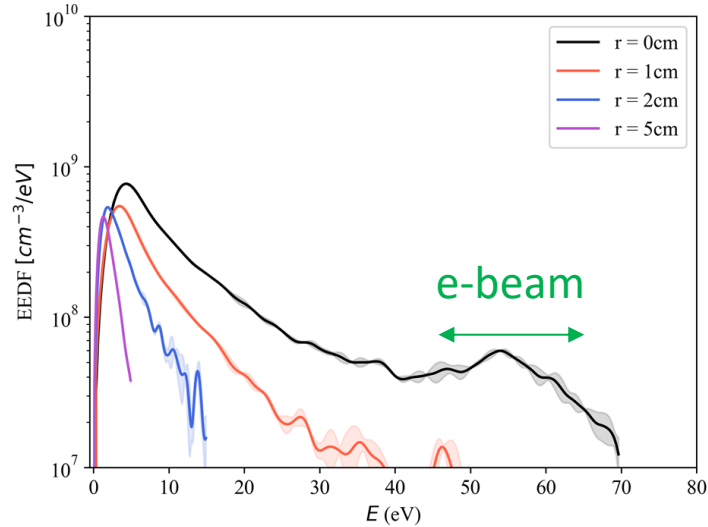
- Argon, 0.1 mtorr, 100 Gauss, 55 V
- Repeller mode
- Time-averaged measurements



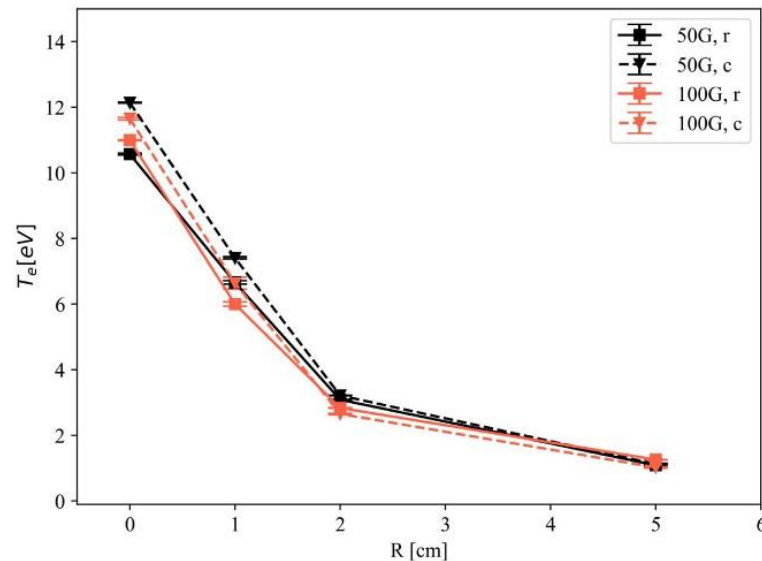
- Radial outward flux of ions (against E-field)
- Maximum ion energy, $\varepsilon_i < 1 \text{ eV}$

Answer: cold electrons and very low energy ions

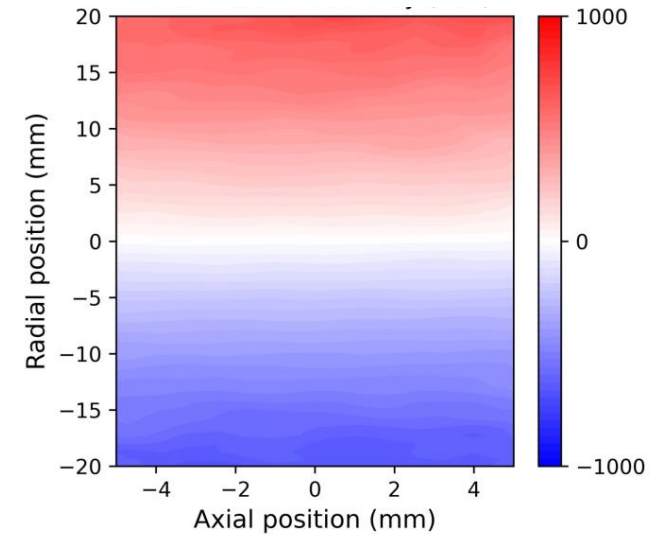
- Electron energy distribution function (EEDF)



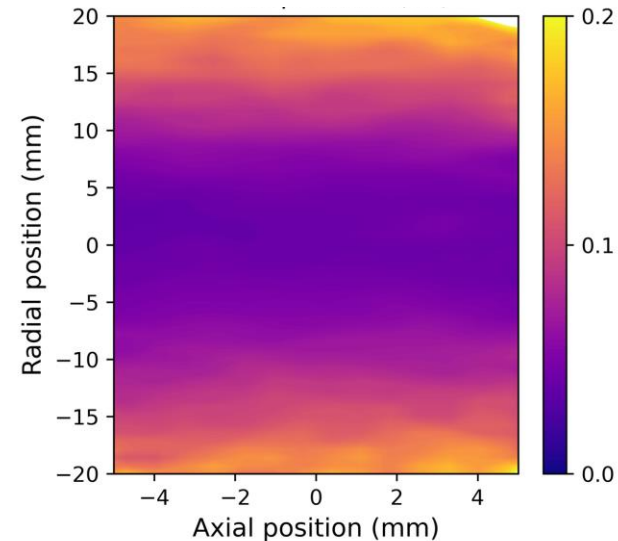
- Electron temperature



- Radial ion velocity, m/s



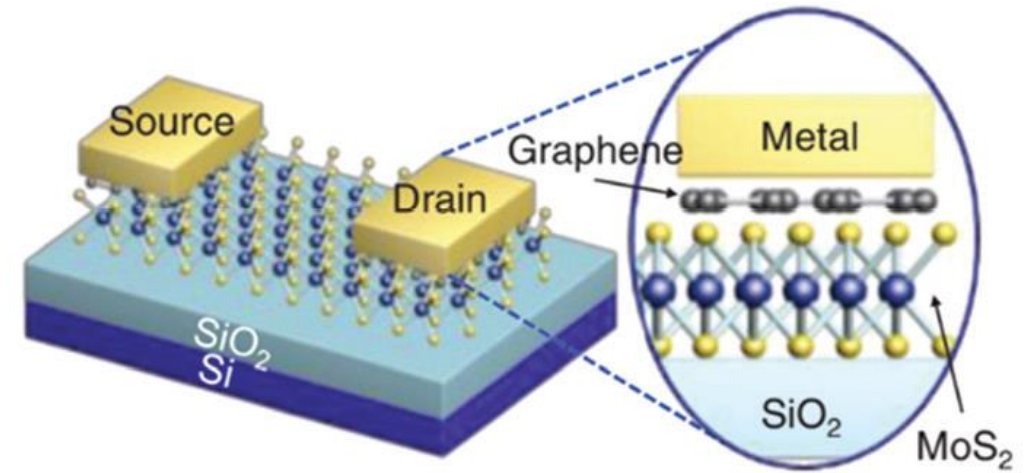
- Ion temperature in R, eV



Motivation: *microelectronics*

- **2D materials for future nanoelectronics**

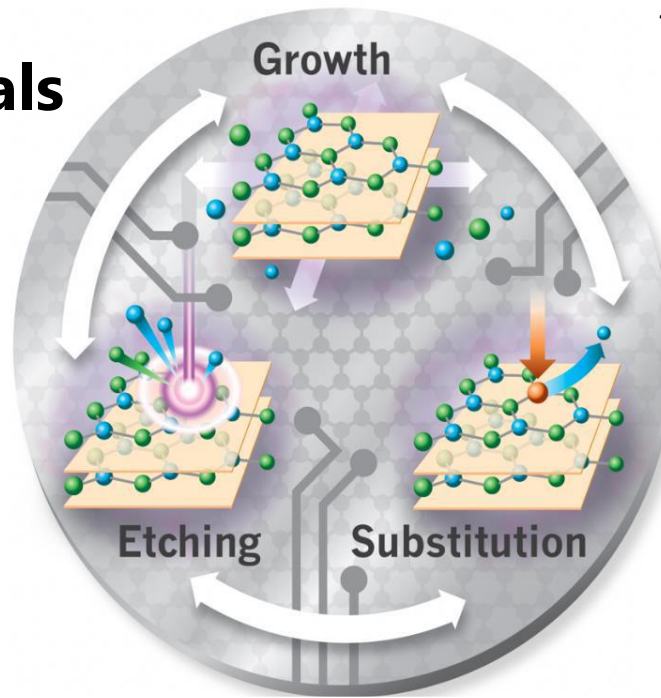
M. C. Lemme, et al., Nat. Commun. 13, 1392 (2022)



FET transistor with 2D materials (MoS₂, graphene)

Source: W. Liao et al., Nanoscale Horiz. 5, 787 (2020)

- **Can plasma enable 2D materials for HVM of 2D electronics?**

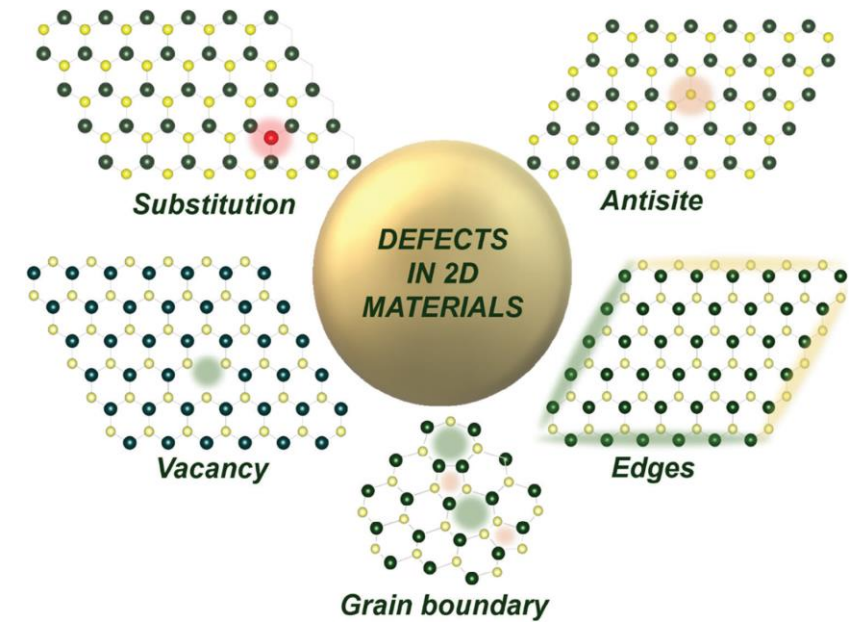


DOE-funded PlasMat2D Project

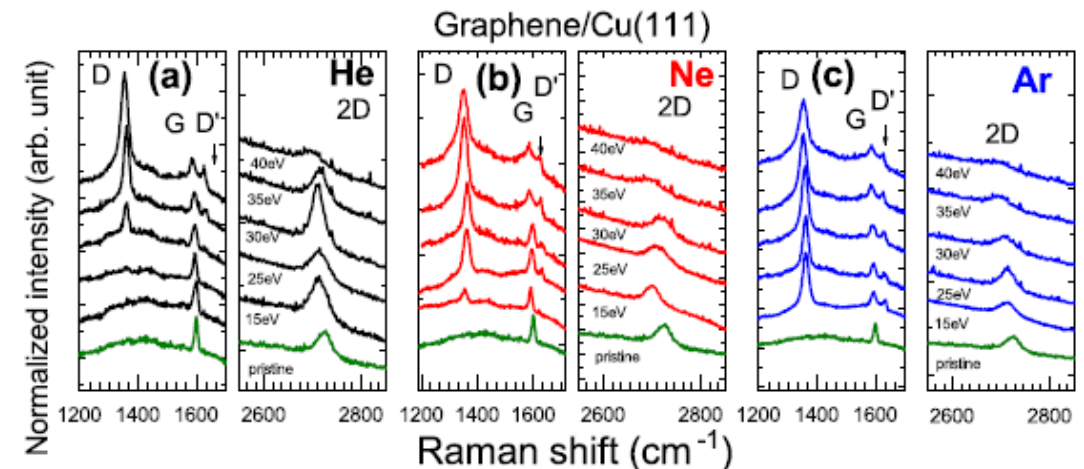
PPPL (lead)
Princeton
Michigan
UCLA
Houston
IBM

Plasma-induced damage to 2D materials: *graphene*

- 2D materials inherently sensitive to lattice defects¹
 - Effects on properties, and nanodevice performance
 - Wanted** vs **Unwanted**
- Defects by ions from the plasma:
 - Ion accelerated in the sheath to a floating substrate:
$$\varepsilon_i \approx T_e \ln \left(\frac{1}{0.61} \sqrt{\frac{M_i}{2\pi m_e}} \right)$$
 - For $T_e \sim 5 \text{ eV}$ **Argon** ion energy, $\varepsilon_i \approx 25 \text{ eV}$
- Displacement energy threshold for C-atom in graphene,² $\varepsilon_d \approx 22 \text{ eV}$
 - Disorder and defects observed at $\sim 15 \text{ eV}$ (bottom fig.) and predicted for even lower energies.³



¹Telkhozhayeva and Girshevitz, *Adv. Funct. Mater.* **34**, 2404615 (2024)



²Kotakoski et al., *Phys. Rev. B* **82**, 113404 (2010)

³R. Villarreal et al., *Carbon* **203**, 590 (2023)

Ion-induced lattice damage to 2D Materials: *TMD*

- DFT and MD predict even more challenging situation for plasma-exposed **Transition Metal Dichalcogenides** (TMDs) – top figure for defects MoS_2 .⁴
- In addition to ion energy, relevant defects and disorders depend on ion incident angle and dose.⁵

Experiments

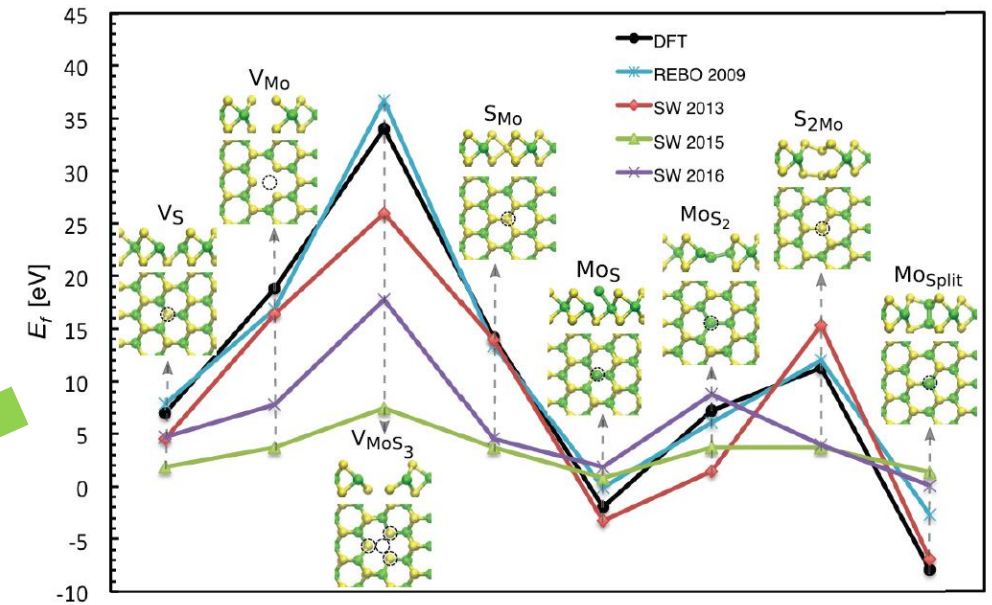
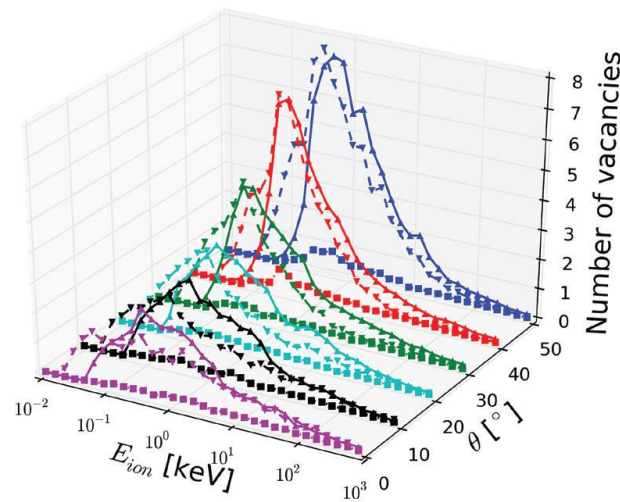
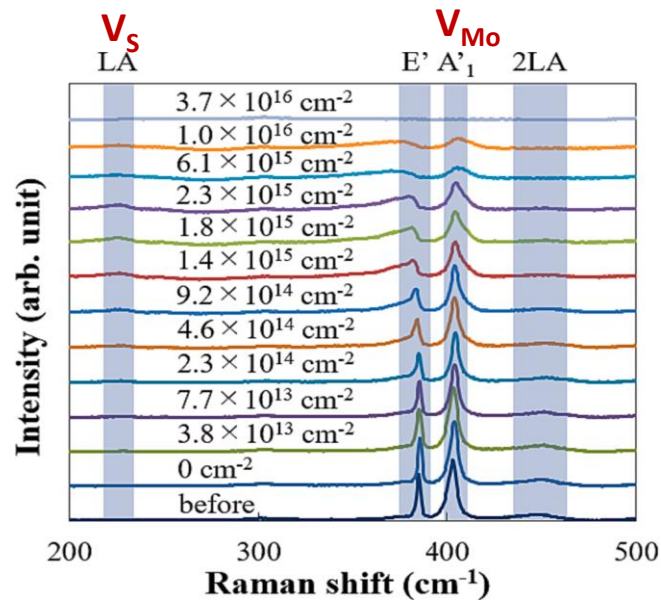


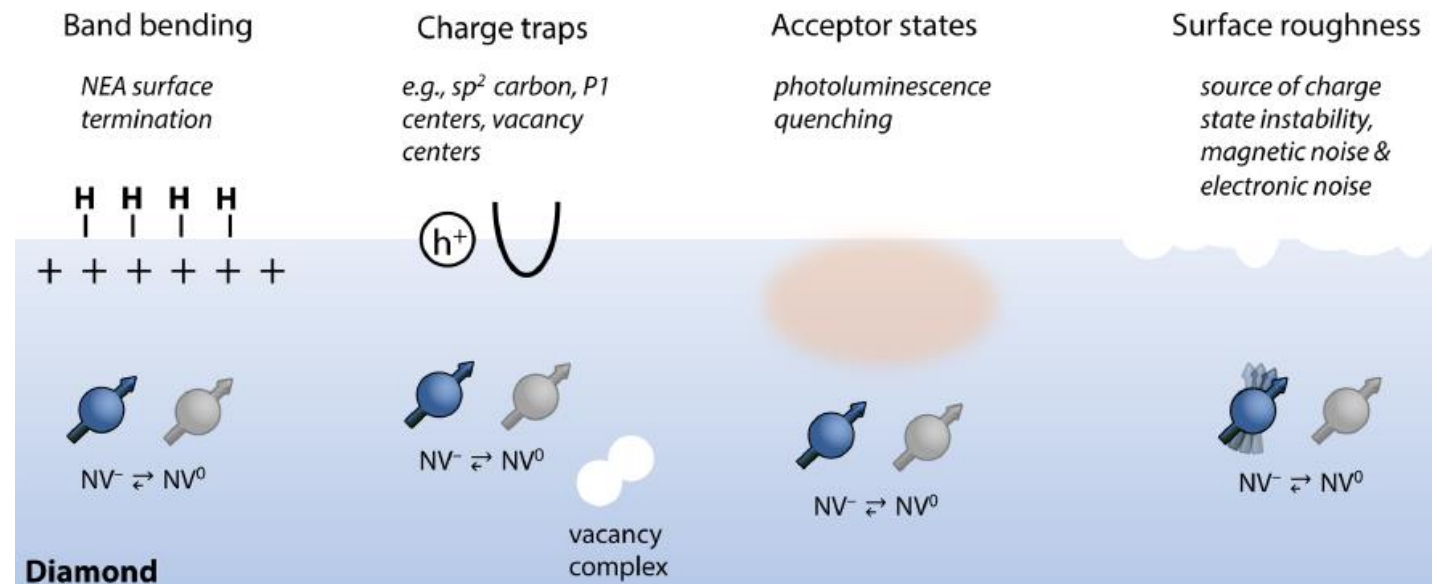
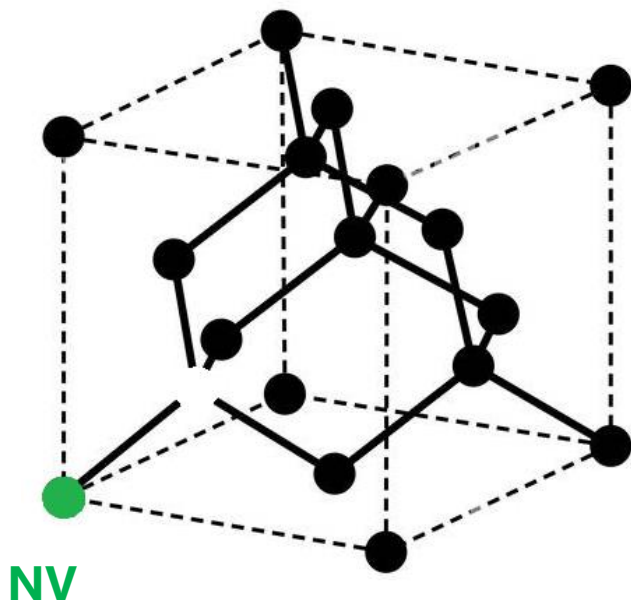
Figure 2. Comparison between formation energies of various type of defects calculated using DFT and empirical potentials. Different types of defects in MoS_2 -ML, from left: vacancies (I)–(III), antisites (IV)–(VII), and the Mo–Mo split interstitial (VIII). Black dashed circles show the position of the defect.

⁴ Ghorbani-Asl et al., 2017 2D Mater. 4 025078 (2017)

To meet the extreme sensitivity and precision demands of 2D material processing, alternative plasma sources are needed to minimize damage while enabling atomic-scale control.

Motivation: QIS

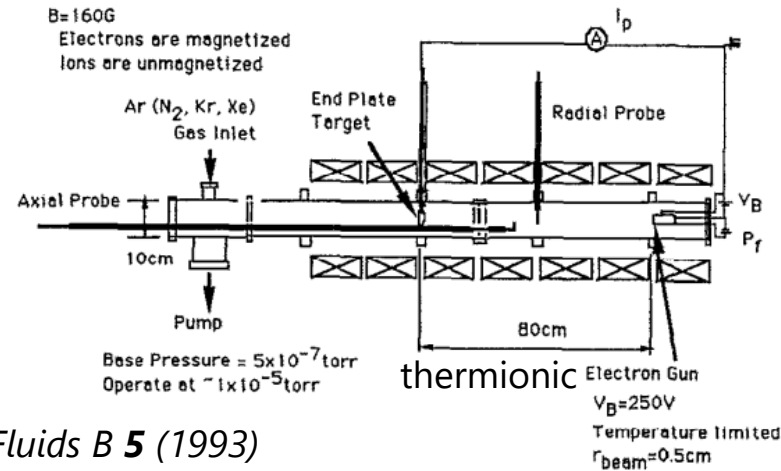
- The nitrogen-vacancy (NV)- center and silicon-vacancy (Si-V) are color centers in diamond with promising applications in quantum information and quantum sensing.
- The stability of the NV- state has been a limitation for their use.
 - Proper surface termination can mitigate this issue!
- A nitrogen termination is an appealing candidate.



Relevant E×B plasma systems

- Thermionic cathode

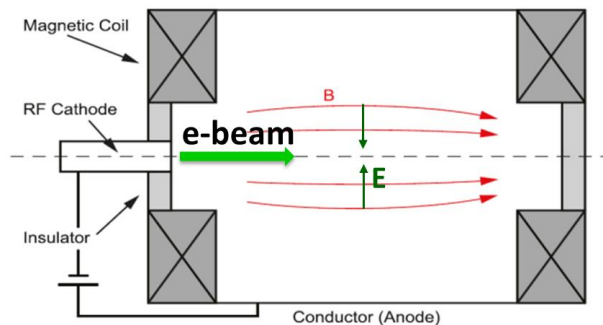
0.01-10 mtorr
10-1000 eV
~ 1-10⁴ mA/cm²



Sakawa, Chen et al., *Phys. Fluids B* **5** (1993)
Chopra and Raitses, *Appl. Phys. Lett.* **126**, (2025)

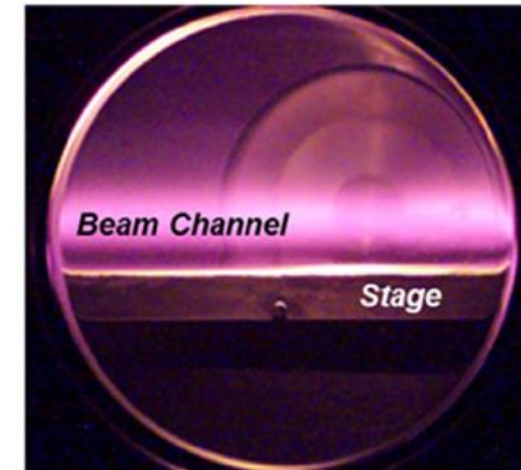
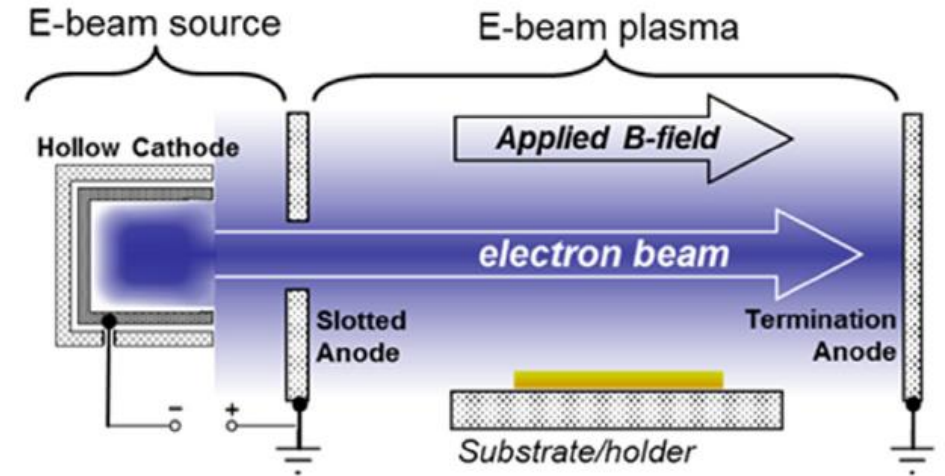
- RF plasma cathode

0.1-10 mtorr
< 60 eV
~ 10³ mA/cm²



Raitses, Kaganovich, Smolyakov et al., *34th IEPC* (2015)
Rodriguez et al., *Phys. Plasmas* **26** (2019)

- Ion-induced secondary electron emission cathode

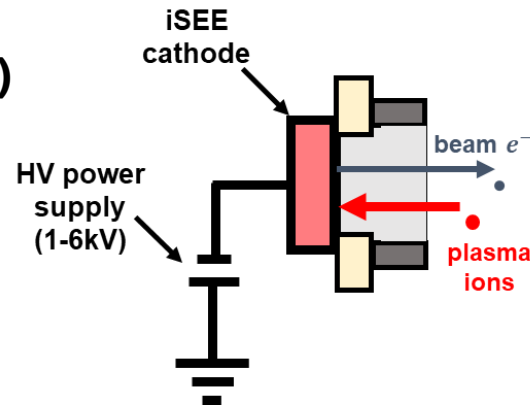


10-100 mtorr
2-4 keV
~ 1-10 mA/cm²

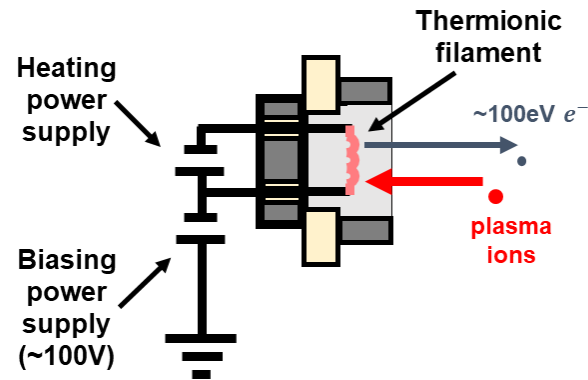
Manheimer et al., *Plasma Sources Sci. Technol.* **9** (2000)
Walton et al., *Surf. Coat. Technol* **186** (2004)

Different electron sources => Different dominant reactions

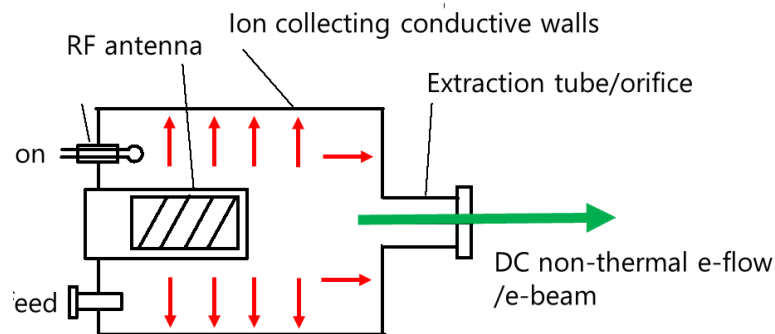
Cold cathode, (iSEE)



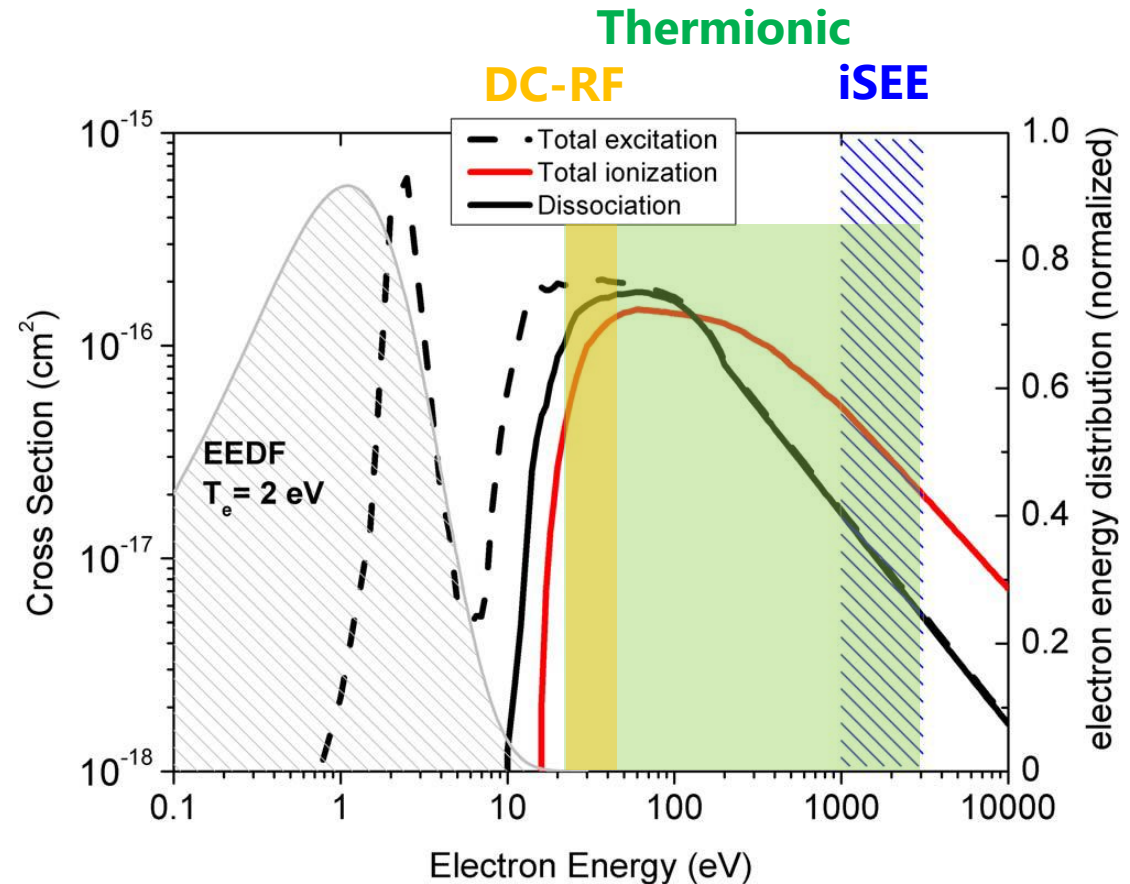
Hot cathode (thermionic)



DC-RF cathode



From Ref. *, Electron impact excitation, dissociation, and ionization cross sections for N_2



* Adapted from S. Walton et al., *Surf. Coat. Technol* **186** (2004)

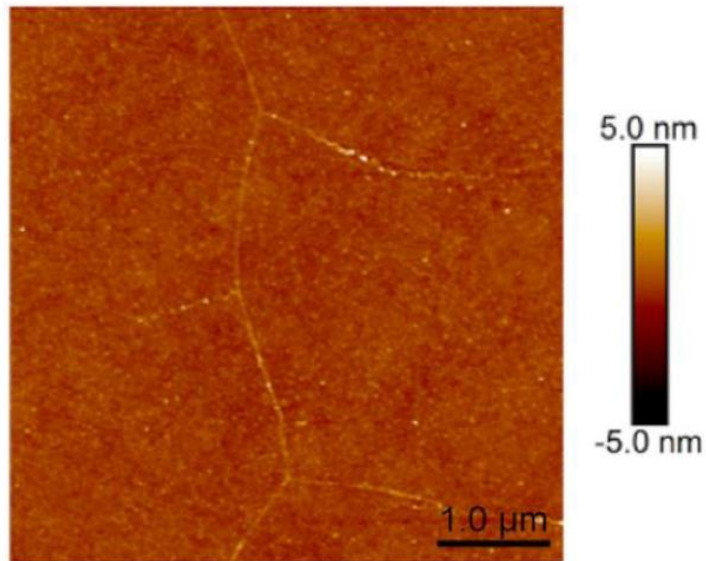
Low temperature $E \times B$ plasma in relevant systems

| Property | Value |
|-------------------------------|----------------------------------------------------------------------------------------------------------------------------------------------|
| Gases | Ar, Kr, Xe, H ₂ , N ₂ , O ₂ , CF ₄ , NF ₃ , CO ₂ , CH ₄ ,... |
| Gas pressure, mtorr | 10 ⁻¹ -10 ² |
| B-field, Gauss | 10-10 ² |
| Electron source, eV | 10-10 ³ |
| E-source current, mA | 1-10 ³ |
| λ_e/L_{ch} | > 1 |
| $v_{in}, v_{CEX}, v_i/f_{ci}$ | ~ 1 |
| $r_{L,e}/R_{ch}$ | $\ll 1$ |
| $r_{L,i}/R_{ch}$ | ≤ 1 |

- Weakly collisional
- Partially ionized
- Partially magnetized

Damageless processing of 2D materials and diamond

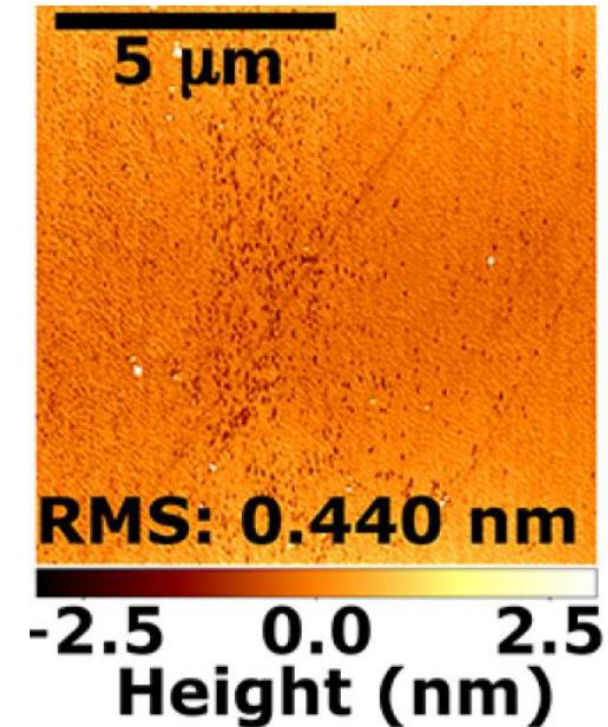
Graphene hydrogenation



Nearly 40% of H coverage

Zhang et al. *Carbon* **2021**, 177, 244

Diamond hydrogenation



Pederson et al. *Phys. Rev. Mat.* **2024**, 8, 036201

Summary

Role of Magnetic Fields

- Constrain electrons $\perp B$, free flow $\parallel B \rightarrow$ higher density, energy control, uniformity

Magnetically-enhanced Sources

- Sputtering magnetrons, e-beam $E \times B$ plasmas, DC Hall/anode-layer ion sources
- *Not covered in this lecture:* ECR & helicon RF, CCPs with applied B-field

Cross-Field Transport and Selected Instabilities

- Anomalous diffusion, gradient-drift instabilities (“spokes”) \rightarrow can heat ions
- Mitigated via segmented electrodes & active boundary control, pressure

Electron-beam generated $E \times B$ plasmas for processing of ion sensitive materials

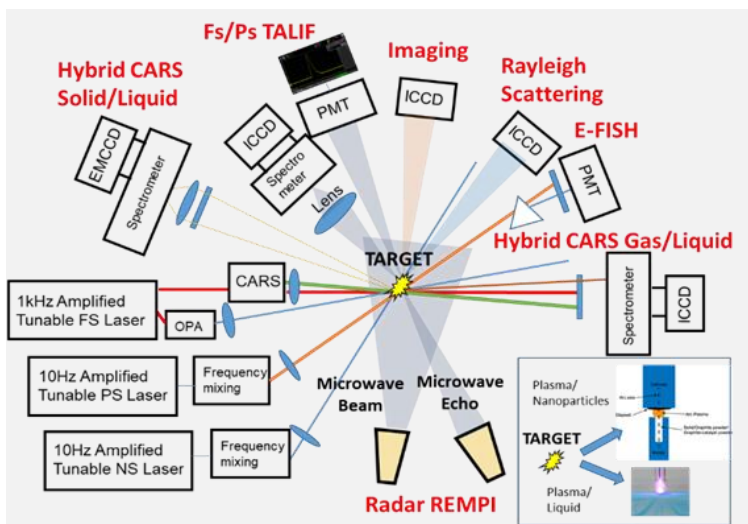
- Graphene hydrogenation ($\approx 38\%$ H coverage)
- Diamond H/N-passivation for color-center preservation
- Emerging applications: TMDs & perovskites



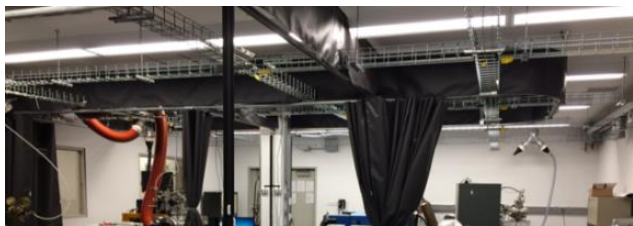
PCRF

Princeton Collaborative Research Facility (PCRF)

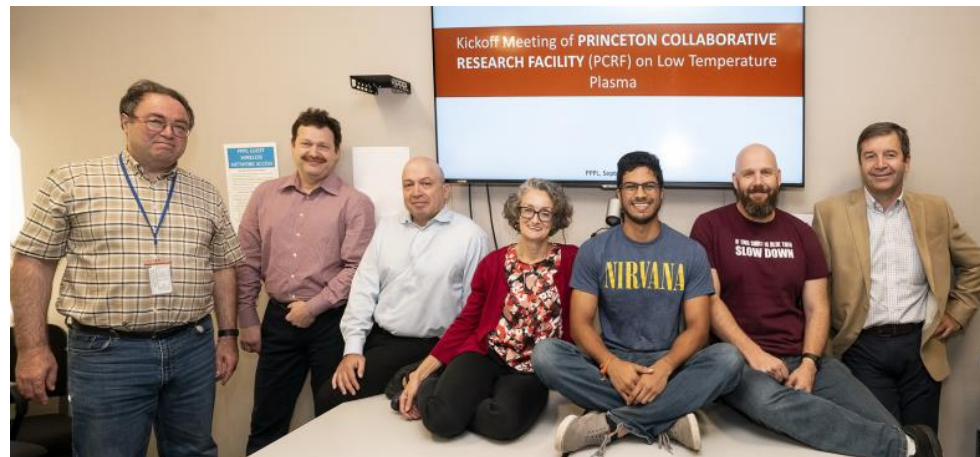
Advanced diagnostics of plasma, gas flow, nanoparticles, plasma-surface interactions



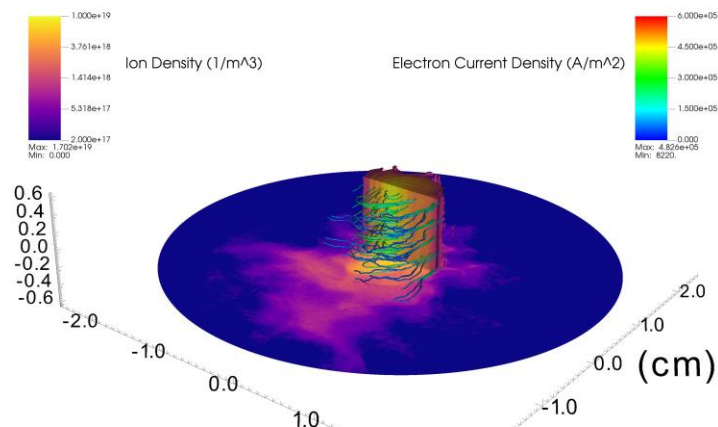
Facilities at PPPL and Princeton
> 5000 sq.ft and more coming



Experts in plasma theory, computational, experiments and diagnostics

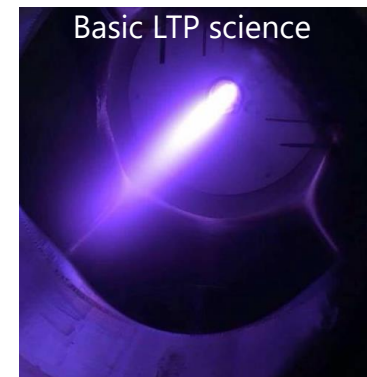


Advanced computational resources: 2D, 3D codes, HPC: CPU-GPU hybrid architecture with open-source codes



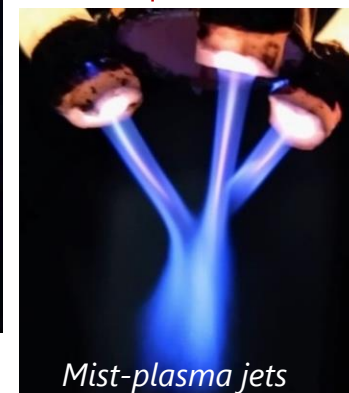
3-D PIC: ExB plasma structures

Wide range of plasma sources for basic and applied research

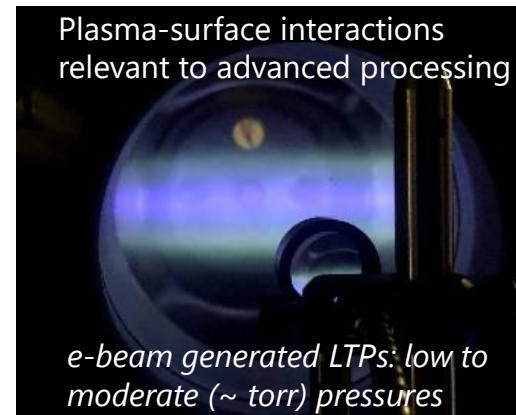


Low pressure ExB plasma

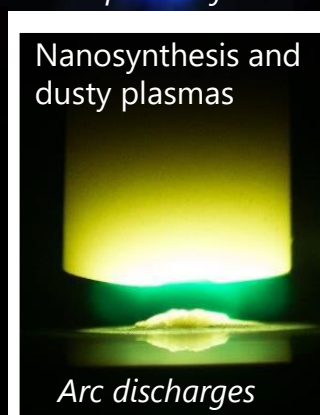
Plasma-liquid interactions



Mist-plasma jets



e-beam generated LTPs: low to moderate (~ torr) pressures



Arc discharges

Since 2019, 125 user projects
<http://pcrf.pppl.gov>

Acknowledgement

- Selected lecture materials courtesy Andrei Smolyakov, Matjaž Panjan, Mikhail Tyushev, Mina Papahn Zadeh, Alex Perel, Igor Koganovich, Rod Boswell, Hokuto Sekine, Panagioitis Svarnas
- PPPL ExB group: Ivan Romadanov, Nirbhav Chopra, Sunghyun Son, and Emma Devin
- The work was supported by the US DOE under Contract No. DEAC02-09CH11466 and by the Air Force Office of Scientific Research
- Research on 2D materials is based partially upon work supported by the U.S. Department of Energy, Office of Science, Fusion Energy Sciences and Basic Energy Sciences, as part of the Extreme Lithography & Materials Innovation Center (ELMIC), a Microelectronics Science Research Center (MSRC) through the Plasma-enabled 2D Materials project at the Princeton Plasma Physics Laboratory (PPPL), under contract number No.DEAC02-09CH11466.
- <http://pcrf.ppp.gov>